Geological Society of America
Special Paper 377
2004

Proterozoic metamorphism of the Tobacco Root Mountains, Montana

John T. Cheney
Department of Geology, Amherst College, Amherst, Massachusetts 01002, USA

John B. Brady
Department of Geology, Smith College, Northampton, Massachusetts 01063, USA

Kara A. Tierney
Kathleen A. DeGraff
Heidi K. Mohlman
Jessica D. Frisch
Christine E. Hatch
Michael L. Steiner
Department of Geology, Amherst College, Amherst, Massachusetts 01002, USA

Sarah K. Carmichael
Robin G.M. Fisher
Department of Geology, Smith College, Northampton, Massachusetts 01063, USA

Carrie B. Tuit
Beloit College, Beloit, Wisconsin 53511, USA

Kurt J. Steffen
Carleton College, Northfield, Minnesota 55057, USA

Pamela Cady
Josh Lowell
Colorado College, Colorado Springs, Colorado 80903, USA

LeAndra L. Archuleta
Jillian Hirst
Pomona College, Claremont, California 91711-6339, USA

Karl W. Wegmann
Whitman College, Walla Walla, Washington 99362, USA

Brian Monteleone
College of Wooster, Wooster, Ohio 44691-2363, USA

ABSTRACT

Textures and mineral assemblages of metamorphic rocks of the Tobacco Root Mountains are consistent with metamorphism of all rocks during the Big Sky orogeny (1.77 Ga) at relatively high pressure (*P* >1.0 GPa) followed by differential

Cheney, J.T., Brady, J.B., Tierney, K.A., DeGraff, K.A., Mohlman, H.K., Frisch, J.D., Hatch, C.E., Steiner, M.L., Carmichael, S.K., Fisher, R.G.M., Tuit, C.B., Steffen, K.J., Cady, P., Lowell, J., Archuleta, L.L., Hirst, J., Wegmann, K.W., and Monteleone, B., 2004, Proterozoic metamorphism of the Tobacco Root Mountains, Montana, *in* Brady, J.B., Burger, H.R., Cheney, J.T., and Harms, T.A., eds., Precambrian geology of the Tobacco Root Mountains, Montana: Boulder, Colorado, Geological Society of America Special Paper 377, p. 105–129.

reequilibration on a clockwise *P-T* path at lower pressures (0.6–0.8 GPa). The highest pressures are documented by coarse-grained kyanite and orthopyroxene in aluminous orthoamphibolites, which require $P \geq 1.0$ GPa. Other higher-pressure mineral assemblages of note include kyanite + orthoamphibole and kyanite + K-feldspar. Abundant textural evidence for partial melting in pelitic and basaltic rocks includes leucosomes, very large (several cm across) porphyroblasts of garnet, and an absence of primary (foliation-defining) muscovite. Partial to complete overprinting of the coarse-textured, high-pressure assemblages by lower-pressure assemblages and textures occurred across the Tobacco Root Mountains, especially where assisted by deformation and the availability of water. In aluminous rocks, sillimanite bundles typically replace kyanite, and garnet may be rimmed by cordierite + orthopyroxene symplectite or, in quartz-absent rocks, sapphirine + spinel + cordierite symplectite. Orthoamphibolites with partial pseudomorphs of garnet by cordierite are common. Garnet necklaces surround orthopyroxene in orthopyroxene-plagioclase gneisses, whereas orthopyroxene + plagioclase pseudomorphs of garnet occur in nearby hornblende amphibolites. These features appear to require nearly isobaric cooling at pressures near 0.8 GPa, followed by nearly isothermal decompression at temperatures near 700 °C. The resulting *P-T* path is believed to be the result of tectonic denudation late in the orogenic cycle. Quartz-plagioclase-garnet-hornblende amphibolites occur throughout the Tobacco Root Mountains. Near-rim mineral compositions from these rocks have been used to calculate *T*s of 650–750 °C at *P*s of 0.7–0.9 GPa across the terrane. There is no systematic variation in calculated *P* and *T* between units nor geographically within units; differences appear to reflect variations in thermometer closure possibly due to the availability of water during cooling. Field relations involving metamorphosed mafic dikes, as well as geochronological data from monazite and zircon, demonstrate that some rocks were first metamorphosed at high temperatures and pressures at 2.45 Ga. However, we have not identified mineral assemblages that can be assigned unequivocally to this earlier event.

Keywords: Tobacco Root Mountains, Precambrian, metamorphism, *P-T*-t path.

INTRODUCTION

The metamorphic history of the Tobacco Root Mountains has been studied by a number of previous workers (e.g., Tansley et al., 1933; Reid, 1957, 1963; Root, 1965; Burger, 1966, 1969; Hess, 1967; Gillmeister, 1972b, 1972a; Cordua, 1973; Hanley, 1975, 1976; Friberg, 1976; Immega and Klein, 1976; Vitaliano et al., 1979, see reprinted map and text accompanying this volume; Hanley and Vitaliano, 1983). Many of the important features were first elucidated by Reid (1963) in a paper summarizing his careful field and petrographic work on the northern portion of the range. Reid (1963) postulated the occurrence of "three major metamorphic episodes" (*a*, *b*, *c*) and distinguished five deformations (1–5). In unraveling this history, Reid (1963, p. 293) emphasized the significance of the "metabasalt dikes and sills which cut foliation, tight isoclinal folds, migmatite patterns, and other structures of an older metamorphism *a* of unknown but probably high grade." Previous workers (Tansley et al., 1933) called for two metamorphisms based on their interpretation that the Cherry Creek metasediments (our Indian Creek Metamorphic Suite; see below) contained boulders of Pony gneiss (our Pony–Middle Mountain Metamorphic Suite) and apparently ignoring the constraints of the metamorphosed basalt dikes and sills (our MMDS).

Reid (1963, p. 297) argues that tight, isoclinal folding of compositional layering (deformation no. 1) and an axial plane schistosity occurred during metamorphism *a*, but that the "mineral assemblages of metamorphism *a* have been completely destroyed by later metamorphic recrystallization." He calls for the intrusion of the MMDS after metamorphism *a*, because they crosscut its foliation and isoclinal folds (see Figure 1 *in* Brady et al., 2004b, this volume, Chapter 5). Reid's (1963) metamorphism *b* is assigned to the granulite facies based on the presence of hypersthene in mafic rocks. This metamorphism affects all rocks, including the MMDS, with a shearing deformation (deformation no. 2) that first destroys and then reconstitutes the axial plane schistosity of deformation no. 1. His metamorphism *c* is assigned to the amphibolite facies and is based on mineral assemblages that "appear texturally to be superimposed upon the granulite facies assemblages" (Reid, 1963, p. 296). He calls for additional shear deformation (no. 3) during metamorphism *c* because "new hornblende and biotite … grew parallel to the axial planes of the isoclinal folds of deformation no. 1…." In addition to the three main metamorphic events, Reid (1963, p. 300) observed the incomplete development of replacement assemblages belonging to the epidote-amphibolite facies (his "retrogressive metamorphism *d*") and the greenschist facies (his

"retrogressive metamorphism *e*"). Reid's Table 1 lists the important mineral assemblages that support his interpretation.

Subsequent workers have elaborated upon Reid's (1963) analysis, examining rocks in the central and southern portions of the range, giving additional structural and petrographic details, describing additional mineral assemblages, distinguishing a new map unit (our Spuhler Peak Metamorphic Suite) that did not experience metamorphism *a*, reporting mineral compositions, and using mineral compositions to constrain temperatures and pressures of metamorphism. Much of this research was completed under the supervision of Charles Vitaliano by graduate students at Indiana University. Their results are summarized nicely in Vitaliano et al. (1979) and will not be listed again here. We acknowledge our debt to all these scientists, whose detailed maps, theses, and publications made our own studies possible.

Our work on the metamorphism of Tobacco Root rocks began in 1993, has included portions of 17 undergraduate theses (Archuleta, 1994b; Cady, 1994b; Fisher, 1994b; Lowell, 1994a; Tierney, 1994a; DeGraff, 1996a; Hirst, 1996; Mohlman, 1996a; Tuit, 1996c; Wegmann, 1996a; Carmichael, 1998b; Frisch, 1998b; Hatch, 1998b; Monteleone, 1998a; Steffen, 1998b; Steiner, 1999; Rodriguez, 2002), and has been partially documented through a series of abstracts (Archuleta, 1994a; Brady et al., 1998a; Carmichael et al., 1998; Carmichael, 1998a; Cady, 1994a; Cheney et al., 1994, 1996, 1998; DeGraff et al., 1996; DeGraff, 1996b; Fisher, 1994a; Frisch and Cheney, 1998; Frisch, 1998a; Hatch, 1998a; Hatch and Cheney, 1998; Lowell, 1994b; Martin, 1996; Mohlman, 1996b; Mohlman and Cheney, 1996; Monteleone, 1998b; Steffen, 1998a, 1998c; Tierney, 1994a, 1994b; Tuit, 1996a, 1996b; Wegmann, 1996b). Field observations and suites of samples were collected during the summers of 1993, 1995, and 1997, as part of individual projects focusing on one rock unit or rock type. Our analysis builds on previous work by adding new petrographic and chemical data and by using those data to refine the pressure-temperature (*P-T*) path followed during metamorphism.

In this paper and throughout this volume (see Burger, 2004, this volume, Chapter 1), the metamorphic rocks of the Tobacco Root Mountains have been divided into four suites. (1) The Indian Creek Metamorphic Suite consists of many rocks that are clearly metasediments, including quartzite, marble, iron formation, and aluminous schist, but also includes rocks that are meta-igneous, including amphibolite and quartzofeldspathic gneiss. The Indian Creek Metamorphic Suite rocks were called Cherry Creek metamorphic rocks by Reid (1963) and others. (2) The Pony–Middle Mountain Metamorphic Suite consists principally of quartzofeldspathic gneisses and hornblende amphibolites (see Mogk et al., 2004, this volume, Chapter 2). These are the rocks that Reid (1963) and others have called Pony metamorphic rocks. (3) The Spuhler Peak Metamorphic Suite is a mafic unit that consists principally of amphibolite and Ca-depleted amphibolite, with lesser quartzite and aluminous schist (see Burger et al., 2004, this volume, Chapter 3). These are the rocks that Gillmeister (1972b) called the Spuhler Peak Formation. (4) The metamorphosed mafic dikes and sills (MMDS) are fine-grained, metabasalt rocks that intrude the Pony–Middle Mountain Metamorphic Suite and the Indian Creek Metamorphic Suite, but not the Spuhler Peak Metamorphic Suite (see Brady et al., 2004b, this volume, Chapter 7). They are the metabasalt dikes and sills of Reid (1963) and the metabasites of (Hanley and Vitaliano, 1983). Ultramafic rocks are also present, but these are considered separately in Johnson et al. (2004, this volume, Chapter 4).

All four rock suites have mineral assemblages that record upper amphibolite facies metamorphism. Examples of important observed assemblages are shown in Figure 1 on metamorphic facies diagrams. In the following pages, we use rim compositions of minerals in these assemblages along with several geothermobarometers to calculate temperatures and pressures for the metamorphism that produced them. The upper amphibolite assemblages correspond with metamorphism *c* of Reid (1963), which partly to completely overprints evidence for an earlier metamorphism at higher pressure and at least locally at higher temperature (Reid's metamorphism *b* or metamorphism *a*). Features that appear to have been produced during an earlier event include (1) coarse porphyroblasts of garnet, orthopyroxene, gedrite, and other minerals inconsistent with the grain size of the amphibolite facies minerals; (2) the presence of kyanite (partially pseudomorphed by sillimanite in some cases) with K-feldspar inclusions, requiring a minimum *T* and *P* of 700 °C and 0.8 GPa (Spear et al., 1999); (3) the presence of coarse kyanite and orthopyroxene in the same thin section, requiring a minimum *P* of 1.0 GPa (see below); (4) the presence of orthopyroxene in some rocks of basaltic composition, requiring a minimum *T* of ~800 °C (Pattison, 2003); (5) a variety of corona and necklace textures that are consistent with chemical reactions during decompression at temperatures above 700 °C; and (6) abundant textural evidence for partial melting in pelitic and basaltic rocks, including leucosomes, very large (several cm across) porphyroblasts of garnet, and an absence of primary (foliation-defining) muscovite.

Elsewhere in this volume (Brady et al., 2004b, this volume, Chapter 7; Mueller et al., 2004, this volume, Chapter 9) it has been demonstrated that the MMDS were intruded at 2.07 Ga into the Indian Creek and Pony–Middle Mountain Metamorphic Suites (but not the Spuhler Peak Metamorphic Suite). Because both the MMDS and the Spuhler Peak Metamorphic Suite show evidence of a high-pressure (>0.8 GPa) metamorphism followed by a lower-pressure (~0.6 GPa) metamorphism during the 1.77 Ga Big Sky orogeny, we believe that the Indian Creek and Pony–Middle Mountain Metamorphic Suites also experienced the same two periods of metamorphism. Throughout this paper we will refer to the Big Sky high-pressure event as M1 (Reid's [1963] episode *b*) and the Big Sky lower-pressure event as M2 (Reid's [1963] episode *c*). Metamorphic features that predate M1 textures will be called pre-M1 or M0 (Reid's [1963] episode *a*). In some cases (e.g., monazite growth) we can demonstrate that the pre-M1 features occurred during M0 at 2.45 Ga (Cheney et al., 2004, this volume, Chapter 8); in other cases, we can say with certainty only that the features are pre-M1. Similarly, there are some post-M2 retrograde features of uncertain age (Reid's

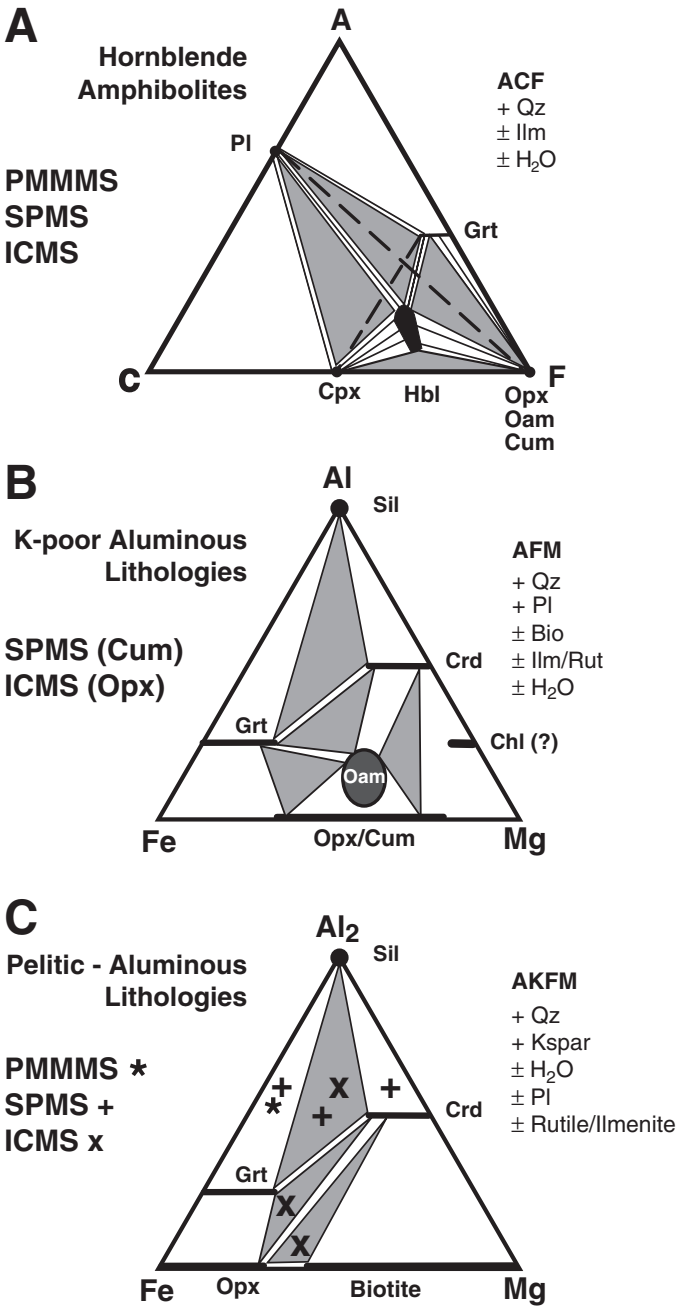

Figure 1. Schematic representation of observed rim assemblages for many Tobacco Root metamorphic rocks are shown as gray triangles on typical metamorphic assemblage diagrams. Additional minerals are listed as projection phases (+) or as possibly present (±). ACF: A—Al, C—Ca, F—Fe + Mg. PMMMS—Pony–Middle Mountain Metamorphic Suite; SPMS—Spuhler Peak Metamorphic Suite; ICMS—Indian Creek Metamorphic Suite; Qz—quartz; Ilm—ilmenite; Opx—orthopyroxene; Oam—orthoamphibole; Cum—cummingtonite; Cpx—clinopyroxene; Hbl—hornblende; Pl—plagioclase; Bio—biotite; Rut—rutile; Sil—sillimanite; Crd—cordierite; Chl—chlorite; Kspar—K-feldspar.

[1963] episodes *d* and *e*). Possibilities include a late Big Sky heating event, heating during ca. 1.4 Ga rifting (Brady et al., 1998b), or contact metamorphic heating during intrusion of the Cretaceous Tobacco Root batholith.

TEMPERATURES AND PRESSURES FROM GEOTHERMOBAROMETERS

Garnet-Hornblende-Plagioclase-Quartz Amphibolites

Amphibolite and amphibolite gneiss are common metamorphic rocks in the Tobacco Root Mountains, occurring in all the major units (Indian Creek Metamorphic Suite, Pony–Middle Mountain Metamorphic Suite, Spuhler Peak Metamorphic Suite, and MMDS). Although textures and modes vary considerably, many samples contain the mineral assemblage hornblende + plagioclase + quartz ± garnet ± augite ± cummingtonite ± biotite along with a variety of other minerals in minor proportions. We have used chemical data from these rocks along with the garnet-hornblende geothermometer of Graham and Powell (1984) and the garnet-hornblende-plagioclase-quartz (Mg) geobarometer of Kohn and Spear (1990) to evaluate metamorphic conditions across the Tobacco Root Mountains using a consistent mineral assemblage.

Chemical data were collected for the critical minerals in rocks with a great variety of textures and a range of bulk composition. See Cady (1994b), DeGraff (1996a), Mohlman (1996a), Wegmann (1996a), Carmichael (1998b), Frisch (1998b), and Steffen (1998b) for petrographic details. In most rocks, hornblende and clinopyroxene (if present) are chemically homogeneous. Plagioclase may be slightly zoned or homogenous. No consistent zoning pattern was observed, except in the MMDS where the anorthite content of plagioclase increases slightly toward the rims of grains, by up to 5 mol%. Garnet grains show only moderate chemical zoning. In the Pony–Middle Mountain and Indian Creek Metamorphic Suites, zoning of Ca in garnet is patchy in some samples. Ca zoning is balanced principally by Fe zoning, with Mg and Mn comparatively unzoned. We interpret this chemical signature as growth of new garnet at 1.77 Ga on old garnet cores in rocks that also experienced metamorphism at 2.45 Ga. In the Spuhler Peak Metamorphic Suite, zoned garnets typically show increasing Mg and decreasing Ca from core to rim, with an Fe increase at the rim. We interpret this zoning as prograde growth zoning during the 1.77 Ga metamorphism, with a rim modified during cooling. Garnets in the MMDS are homogeneous and small (0.1–0.2 mm), possibly recording growth at comparatively high temperature in these dry rocks.

Typical chemical analyses for garnet, plagioclase, and hornblende from one sample each of the four major units are given in Table 1. Chemical analyses of minerals were obtained principally by energy-dispersive X-ray fluorescence (EDS-XRF) at Amherst College and Smith College using Link/Oxford EDS hardware and software and ZAF corrections based on mineral standards. Garnet compositions are 50%–60% almandine and 20%–30%

TABLE 1. GARNET-HORNBLENDE-PLAGIOCLASE-CLINOPYROXENE ANALYSES

Sample	KJS-9a	KJS-9a	KJS-9a	KJS-9a	KJS-9a	JDF-38a2	JDF-38a2	JDF-38a2	JDF-38a2	JDF-38a2	JDF-38a2
Unit	SPMS	SPMS	SPMS	SPMS	SPMS	ICMS	ICMS	ICMS	ICMS	ICMS	ICMS
UTM	504045N	504045N	504045N	504045N	504045N	504402N	504402N	504402N	504402N	504402N	504402N
12T	042018E	042018E	042018E	042018E	042018E	041338E	041338E	041338E	041338E	041338E	041338E
Mineral	Grt core	Grt rim	Hbl unzoned	Pl core	Pl rim	Grt core	Grt rim	Hbl unzone	Pl core	Pl rim	Cpx unzoned
Oxide (wt%)											
SiO_2	38.37	38.48	45.94	49.18	50.43	38.52	37.96	42.28	53.00	56.23	52.79
Al_2O_3	21.02	21.19	12.18	31.94	31.30	20.79	20.53	12.43	29.15	27.47	2.03
TiO_2	N.D.†	N.D.	1.27	N.D.	N.D.	0.08	0.23	1.67	0.03	0.00	0.21
MgO	5.03	5.47	12.34	N.D.	N.D.	3.41	3.44	8.30	0.07	0.00	10.47
FeO*	23.40	25.14	12.43	0.00	0.26	24.25	24.29	18.18	0.25	0.57	13.73
MnO	2.40	1.96	0.16	N.D.	N.D.	1.15	1.35	0.09	0.00	0.00	0.15
CaO	8.89	7.14	11.10	15.23	13.65	11.82	11.46	11.59	11.40	8.10	20.90
Na_2O	N.D.	N.D.	0.92	2.58	3.15	N.D.	N.D.	1.65	4.65	6.18	0.66
K_2O	N.D.	N.D.	0.43	0.34	0.34	N.D.	N.D.	0.78	0.35	0.91	0.01
Total	99.11	99.38	96.77	99.27	99.13	100.02	99.26	96.97	98.90	99.46	100.95
Elements per Formula											
O	12	12	23	8	8	12	12	23	8	8	6
Si	3.02	3.02	6.72	2.26	2.31	3.02	3.01	6.43	2.43	2.55	1.95
Al	1.95	1.96	2.10	1.73	1.69	1.92	1.92	2.23	1.57	1.47	0.10
Ti	N.D.	N.D.	0.14	N.D.	N.D.	0.00	0.01	0.19	0.00	0.00	0.01
Mg	0.59	0.64	2.69	N.D.	N.D.	0.40	0.41	1.88	0.01	0.00	0.63
Fe	1.54	1.65	1.52	0.00	0.01	1.59	1.61	2.31	0.01	0.02	0.35
Mn	0.16	0.13	0.02	N.D.	N.D.	0.08	0.09	0.01	0.00	0.00	0.01
Ca	0.75	0.60	1.74	0.75	0.67	0.99	0.97	1.89	0.56	0.39	0.91
Na	N.D.	N.D.	0.26	0.23	0.28	N.D.	N.D.	0.49	0.41	0.54	0.07
K	N.D.	N.D.	0.08	0.02	0.02	N.D.	N.D.	0.15	0.02	0.05	0.00
Total Cations	8.01	8.00	15.27	4.99	4.98	8.00	8.02	15.58	5.01	5.02	4.03
Mg/Mg + Fe)	0.28	0.28	0.64			0.20	0.20	0.45			0.64

(continued)

grossular. Plagioclase is much more variable, ranging from 25% to 75% anorthite. Hornblende has a significant edenite component and, except for Spuhler Peak Metamorphic Suite samples, has more Fe than Mg. These mineral compositions meet the criteria listed by Kohn and Spear (1990) for use with their geobarometer. Calculated temperatures and pressures using rim compositions for the samples in Table 1 and other rocks are shown in Figure 2. Because there is little chemical zoning, core compositions yield similar results. Most temperatures are in the interval 600–750 °C. Pressures range from 0.5 to 0.9 GPa. Uncertainties in the individual data points are based on observed variations of the mineral compositions in single thin sections. Friberg (1994) reported similar pressures and temperatures for Spuhler Peak Metamorphic Suite amphibolites using this assemblage. These conditions are in the kyanite zone, although nearby pelitic rocks contain sillimanite. This may mean that the thermobarometer is inaccurate, but we suspect that reequilibration of the relevant minerals was not achieved during the decompression that produced the sillimanite (see below).

Although there is a considerable range of calculated temperatures and pressures, we can find no system to the scatter. We were not able to document geographic regions with consistently higher temperatures and/or pressures nor to find any regular variation with sample elevation (Frisch, 1998b). Similarly, there seems to be no systematic variation with strain. Rodriguez (2002) found that amphibolite samples of all fabric types gave kyanite zone temperatures and pressures consistent with those given in Figure 2. We believe that the range in temperatures and pressures shown on Figure 2 results from an array of garnet and hornblende compositions that record the complex reaction history of each sample. This history is differentially preserved in the minerals and includes both retrograde exchange reactions and net transfer reactions. The temperature variation within a given sample is typically on the order of ±25 °C and reflects the chemical homogeneity of the garnet. All iron was treated as ferrous for this analysis. Accordingly some of the inter-sample temperature variation may be due to variation in ferric iron among amphiboles from different samples. Variation in ferric iron does not significantly affect the geobarometer of Kohn and Spear (1990) because the calibration is not strongly dependent on the Mg/Fe ratio of the amphibole. We believe that these temperatures and pressures were recorded in the mineral compositions during a

TABLE 1. GARNET-HORNBLENDE-PLAGIOCLASE-CLINOPYROXENE ANALYSES (*continued*)

Sample	JDF-20a2	JDF-20a2	JDF-20a2	JDF-20a2	JDF-20a2	SKC-1-3a	SKC-1-3a	SKC-1-3a	SKC-1-3a	SKC-1-3a	SKC-1-3a
Unit	PMMMS	PMMMS	PMMMS	PMMMS	PMMMS	MMDS	MMDS	MMDS	MMDS	MMDS	MMDS
UTM	505076N	505076N	505076N	505076N	505076N	504771N	504771N	504771N	504771N	504771N	504771N
12T	041476E	041476E	041476E	041476E	041476E	041498E	041498E	041498E	041498E	041498E	041498E
Mineral	Grt	Grt	Hbl	Pl	Pl	Grt	Grt	Hbl	Pl	Pl	Cpx
	core	rim	unzoned	core	rim	core	rim	unzoned	core	rim	unzoned
Oxide (wt%)											
SiO_2	37.86	36.92	41.46	59.97	58.73	37.61	38.43	42.03	63.33	62.08	52.79
Al_2O_3	20.44	20.10	12.15	24.84	25.59	20.32	20.82	11.61	24.24	25.03	2.03
TiO_2	0.25	0.00	2.14	0.11	0.05	0.05	0.04	2.17	0.04	0.03	0.21
MgO	3.15	2.68	8.18	0.02	0.07	3.37	3.32	7.99	0.01	0.06	10.47
*FeO	27.63	26.90	19.14	0.31	0.43	29.41	29.62	20.01	0.11	0.36	13.73
MnO	3.12	4.21	0.22	0.04	0.01	0.95	0.95	0.05	0.00	0.00	0.15
CaO	7.83	7.79	11.15	6.94	7.67	7.19	7.04	11.18	5.35	6.25	20.90
Na_2O	N.D.	N.D.	1.35	7.51	7.38	N.D.	N.D.	1.77	8.43	8.06	0.66
K_2O	N.D.	N.D.	1.79	0.24	0.12	N.D.	N.D.	0.98	0.21	0.08	0.01
Total	98.60	97.58	99.98	100.05	98.91	100.21	97.79	101.71	101.94	100.95	100.95
Elements per Formula											
O	12	12	23	8	8	12	12	23	8	8	6
Si	3.01	3.00	6.34	2.68	2.63	3.03	3.04	6.42	2.76	2.71	1.98
Al	1.92	1.92	2.19	1.31	1.35	1.93	1.94	2.09	1.24	1.29	0.09
Ti	0.02	0.00	0.25	0.00	0.00	0.00	0.00	0.25	0.00	0.00	0.01
Mg	0.37	0.32	1.86	0.00	0.01	0.40	0.39	1.82	0.00	0.00	0.59
Fe	1.84	1.83	2.45	0.01	0.02	1.98	1.96	2.56	0.00	0.01	0.43
Mn	0.21	0.29	0.03	0.00	0.00	0.06	0.06	0.01	0.00	0.00	0.00
Ca	0.67	0.68	1.83	0.33	0.37	0.62	0.60	1.83	0.25	0.29	0.84
Na	N.D.	N.D.	0.40	0.65	0.64	N.D.	N.D.	0.52	0.71	0.68	0.05
K	N.D.	N.D.	0.35	0.01	0.01	N.D.	N.D.	0.19	0.01	0.00	0.00
Total Cations	8.04	8.04	15.70	4.99	5.03	8.02	7.99	15.69	4.98	5.00	3.99
Mg/(Mg + Fe)	0.17	0.15	0.43			0.17	0.17	0.42			0.58

Note: Data from Carmichael (1998b), Frisch (1998b), Steffen (1998b). SPMS—Spuhler Peak Metamorphic Suite; ICMS—Indian Creek Metamorphic Suite; PMMMS—Pony–Middle Mountain Metamorphic Suite; MMDS—metamorphosed mafic dikes and sills; Grt—garnet; Hbl—hornblende; Pl—Plagioclase; Cpx—Clinopyroxene.

*FeO—total iron as FeO.

†N.D.—no data.

decompression part (M2) of the *P-T* path (see below) following the highest-pressure phase (M1) of the Big Sky orogeny.

Garnet-Clinopyroxene-Hornblende-Plagioclase-Quartz Amphibolites

Some of the amphibolite samples from the Indian Creek Metamorphic Suite, Pony–Middle Mountain Metamorphic Suite, and MMDS have clinopyroxene. See Table 1 for examples of clinopyroxene compositions. Pattison (2003) reviewed experimental and natural data for this assemblage and finds considerable uncertainty regarding its stability. Most examples he reports occur at pressures from 0.7 to 1.2 GPa and from 700 to 800 °C. The assemblage garnet + clinopyroxene + plagioclase + quartz is the basis of the geobarometer of Moecher et al. (1988) and can be used with the garnet-clinopyroxene geothermometer of Powell (1985) to calculate temperatures and pressures. Results of this calculation for representative samples are shown in Figure 3. On average these pressures are higher than those obtained using the hornblende-bearing assemblages for the same rocks. However, the pressures are lowered if ferric iron corrections are made to the analyses, so there may be no significant difference from the hornblende results. Ferric iron is an issue here because calibrations used by Moecher et al. (1988) and Powell (1985) were based on ferric iron–free experimental data, whereas the Kohn and Spear (1990) and Graham and Powell (1984) calibrations were based on natural assemblages that would have contained some ferric iron. Hess and Vitaliano (1990) report similar temperatures and somewhat lower pressures for this assemblage in MMDS samples using different thermobarometer calibrations.

Other thermobarometers were applied to Tobacco Root rocks where the assemblages were appropriate. Aluminosilicate-bearing pelitic rocks are not widely distributed across the Tobacco Root Mountains, and we did not systematically evaluate the thermobarometry in these rocks. Different calibrations of garnet-biotite thermometers were applied to a few samples of

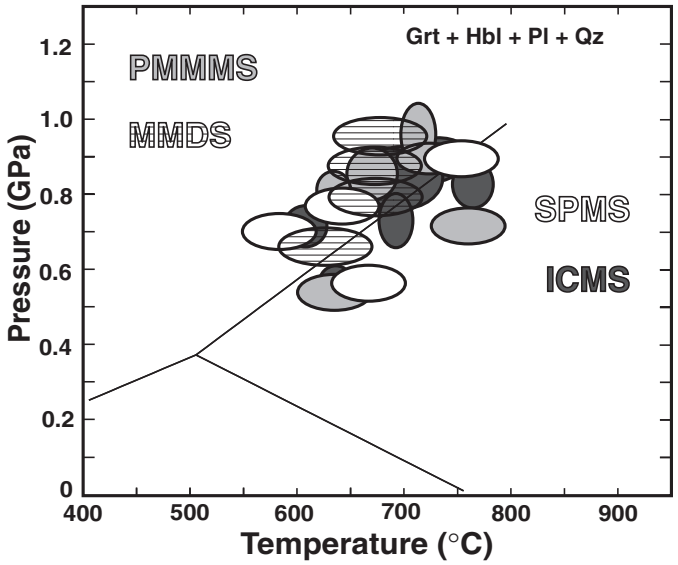

Figure 2. Pressures and temperatures for garnet (Grt) + hornblende (Hbl) + plagioclase (Pl) + quartz (Qz) amphibolites calculated with the Graham and Powell (1984) geothermometer and the Kohn and Spear (1990) geobarometer. Uncertainty ellipses are derived from observed compositional variations of minerals in the samples studied. The aluminosilicate triple point of Holdaway (1971) is shown for reference. PMMMS—Pony–Middle Mountain Metamorphic Suite, MMDS—metamorphosed mafic dikes and sills, SPMS—Spuhler Peak Metamorphic Suite, ICMS—Indian Creek Metamorphic Suite.

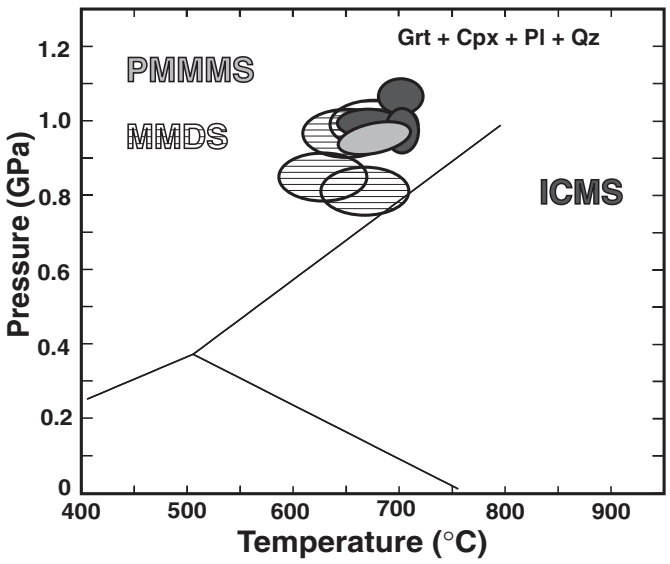

Figure 3. Pressures and temperatures for garnet (Grt) + clinopyroxene (Cpx) + plagioclase (Pl) + quartz (Qz) amphibolites calculated with the Powell (1985) geothermometer and the Moecher et al. (1988) geobarometer. Uncertainty ellipses are derived from observed compositional variations of minerals in the samples studied. No correction was made for possible small quantities of ferric iron. PMMMS—Pony–Middle Mountain Metamorphic Suite, MMDS—metamorphosed mafic dikes and sills, ICMS—Indian Creek Metamorphic Suite.

several rock types where appropriate. The resulting temperatures are typically 25–50 °C lower for the calibration of Patino Douce et al. (1993) than for the calibration of Hodges and Spear (1982). The lower temperatures given by the Patino Douce et al. (1993) geothermometer reflect the correction for the relatively high titanium contents of these biotites. The near-rim (typically within 30 μm of the edge) temperatures from the aluminous rocks are consistent with and overlap those discussed above for the garnet amphibolites (Fisher, 1994b; Monteleone, 1998b). However, garnet-biotite temperatures calculated from hornblende-bearing rocks are generally higher, some by as much as 100 °C (with the Patino Douce et al., 1993, calibration), than hornblende-garnet temperatures from the same rock. Spear and Markussen (1997) reported similar discrepancies for high-grade hornblende-bearing rocks. Reasons for this discrepancy may include different closure temperatures for biotite and hornblende, inappropriate garnet and/or biotite compositions for the thermometer calibrations, or incorrect determination of biotite and amphibole composition as discussed by Spear and Markussen (1997). A number of samples contained orthopyroxene. Although the presence of orthopyroxene in mafic rocks is used to recognize granulite facies conditions, the garnet + orthopyroxene + plagioclase + quartz assemblage yielded temperatures and pressures similar to those of Figures 2 and 3. In sum, geothermobarometers record upper amphibolite facies conditions of 0.5–0.9 GPa and 600–750 °C for rim compositions of mafic rocks throughout the Tobacco Root Mountains. Whatever their detailed metamorphic *P-T* path, it appears that all rocks passed through these conditions. More information about the *P-T* path of these rocks can be obtained from reaction textures in rocks of less common bulk compositions, to which we now turn.

CRITICAL ASSEMBLAGES AND REACTION TEXTURES

Orthoamphibolite

Some of the best evidence for the complex metamorphic history of the Tobacco Root Mountains occurs in aluminous orthoamphibolites, which have preserved a variety of diagnostic mineral assemblages and reaction textures. Coarse-textured (>1 cm) orthoamphibolites are a common and distinctive component of the Spuhler Peak Metamorphic Suite, but orthoamphibolites have also been mapped in the Indian Creek Metamorphic Suite. For example, the highest pressures for Tobacco Root metamorphism are documented by coarse-grained kyanite and orthopyroxene in aluminous orthoamphibolites, which require pressures above ~1.0 GPa as shown in Figure 4. Although we have not observed these minerals in physical contact, they occur in the same thin section and both have the coarse texture that we believe represents growth

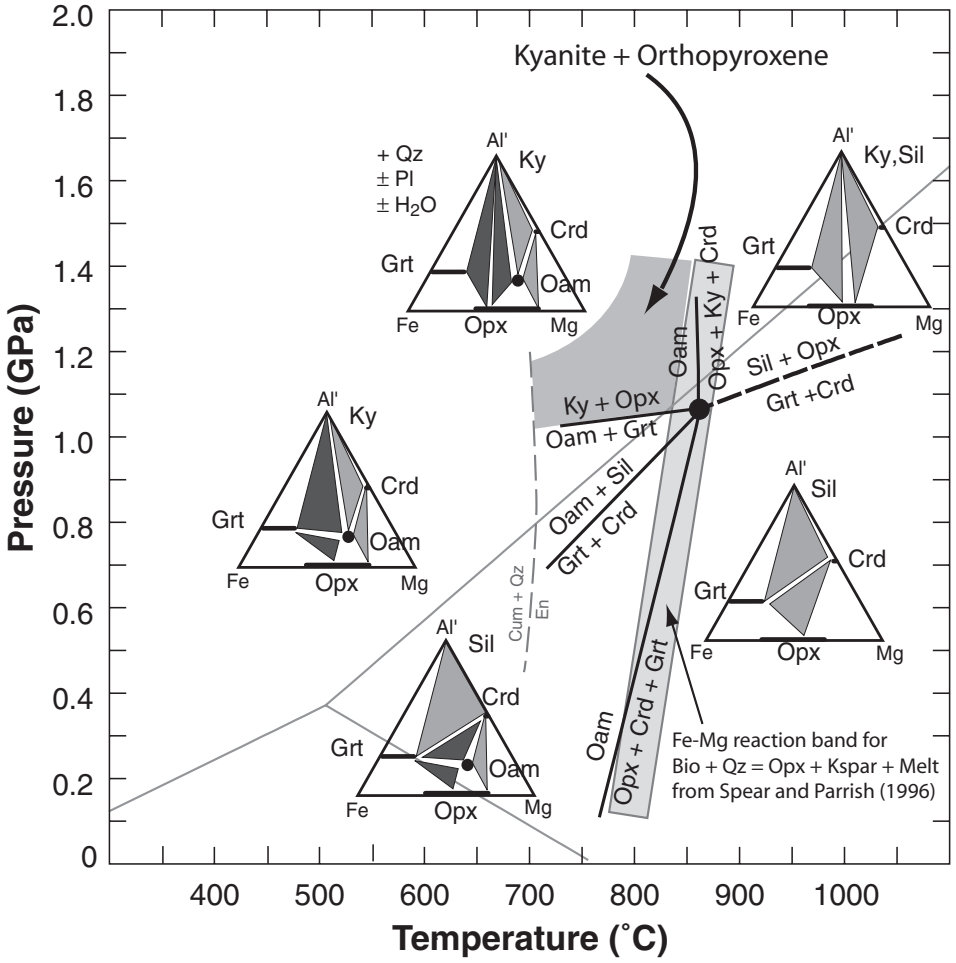

Figure 4. *P-T* diagram showing kyanite + orthopyroxene stability and an invariant point from a schematic petrogenetic grid for cordierite (Crd) + orthoamphibole (Oam) rocks and for garnet (Grt) + orthopyroxene (Opx) + orthoamphibole (Oam) rocks with kyanite (Ky) or sillimanite (Sil). The grid is slightly modified from that of Harley (1985). In particular, the location for the reaction Grt + Crd = Sil + Opx was calculated using the data of Holland and Powell (1998). The other reactions radiating from the invariant point were adjusted to fit the calculated curve. $P_{H_2O} = P_{total}$ is assumed; therefore pressures are maximum values for hydrous cordierite. A band is shown for the reaction biotite (Bio) + Qz = Opx + K-feldspar (Ksp) + Melt for varying Fe/Mg values from Spear and Parrish (1996). The Holdaway (1971) aluminosilicate triple point and the curve (dashed) marking the lower temperature limit of enstatite (En), calculated from the database of Holland and Powell (1998), are shown for reference.

during M1. The range of *P-T* conditions permitted by the coexistence of kyanite + orthopyroxene (Fig. 4) is limited at low pressure by the intersection of the sillimanite + orthopyroxene curve with the kyanite stability field. The low temperature boundary is provided by the low temperature limit of enstatite stability. The absence of orthopyroxene + K-feldspar or orthopyroxene-bearing migmatites in either the aluminous gneisses or the orthoamphibolites and the abundance of biotite in these rocks requires temperatures less than the dehydration melting reaction of Spear and Parrish (1996) for biotite + quartz, as shown in Figure 4.

The important minerals in these rocks can be shown on a modified AFM diagram (Spear, 1993, Chapter 13 therein) that is a projection from quartz, water, and if present, plagioclase. Figure 4 also shows a schematic invariant point and associated chemical reactions for the orthoamphibolites using this modified AFM diagram to illustrate the chemography. The location of the invariant point is modified slightly from Harley (1985) to be consistent with the sillimanite + orthopyroxene curve, located on Figure 4 assuming $P_{H_2O} = P_{total}$ and using the thermodynamic data set of Holland and Powell (1998). The upper stability limit of orthoamphibole for $P_{H_2O} = P_{total}$ as shown on Figure 4 is consistent with observed mineral occurrences in the Tobacco Root Mountains. Because there is abundant orthoamphibole in Tobacco Root rocks, with no textural evidence of its instability at high temperature, we believe the orthoamphibole-out reaction is an upper temperature bound to the *P-T* path.

Garnet-Cordierite Textures

A particularly impressive Spuhler Peak Metamorphic Suite sequence that includes orthoamphibolite with golf ball–sized (1–5 cm across) garnets is well exposed along the ridge running west from Thompson Peak (Fig. 5). The coarse grain size of these rocks, their absence of fabric, and the high concentration of refractory minerals leads us to believe that these rocks underwent partial melting during metamorphism. Many garnet crystals are roughly dodecahedral in form and are red brown in color, except along fractures and in rims where they have the blue gray color of cordierite. Coarse (1 mm) brown biotite flakes may wrap around garnet porphyroblasts, whereas fine, brown green biotite shows no orientation and may be intergrown with cordierite. The orthoamphibole gedrite occurs as euhedral, tabular grains up to 15 cm in length. Many samples have a characteristic play of

Figure 5. Orthoamphibolite with large garnets from the Spuhler Peak Metamorphic Suite along the ridge running west from Thompson Peak. The garnet crystals are replaced partially by cordierite on their margins and along cracks. The hammer in the photo is 33 cm long.

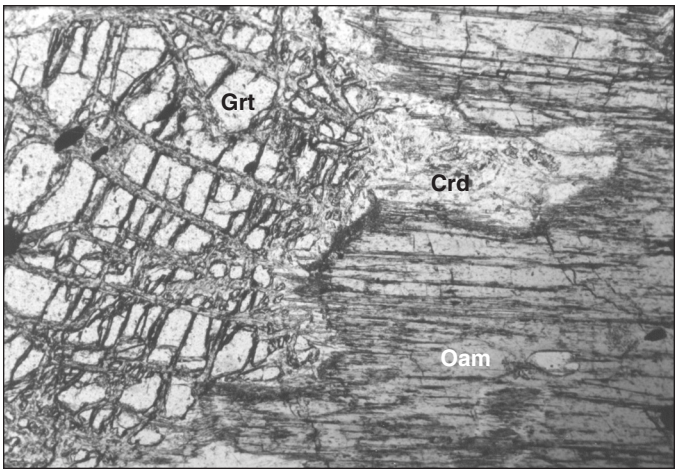

Figure 6. Photomicrograph in plane-polarized light of cordierite (Crd) replacing garnet (Grt) and as a moat between garnet and orthoamphibole (Oam). Sample KAT-44. The field of view is 5 mm wide.

colors due to anthophyllite exsolution lamellae. In thin section, the presence of cordierite can be confirmed by the presence of yellow pleochroic haloes around zircon and monazite inclusions. Cordierite occurs principally as a textural replacement of garnet along fractures and where it is in contact with gedrite (see Fig. 6). Chemical analyses of the minerals in a sample with cordierite are given in Table 2.

The presence of cordierite in equilibrium with garnet and gedrite limits the maximum pressure and temperature to 1.0 GPa and 800 °C (Fig. 4) at $P_{H_2O} = P_{total}$, and to lower temperatures and pressures if $P_{H_2O} < P_{total}$. We believe the introduction of cordierite into the orthoamphibolites begins with the decompression reaction

$$\text{Oam} + \text{Ky} = \text{Grt} + \text{Crd} + \text{H}_2\text{O} \quad (1),$$

where Oam is orthoamphibole, Ky is kyanite, Grt is garnet, and Crd is cordierite. With the addition of Mn and/or Ca in the garnet, discontinuous reaction 1 becomes continuous. As shown in Table 2, the amount of grossular component is less than 2% and the spessartine component is less than 1% for garnet from these rocks. The modal amount of garnet is also much greater than that of cordierite. Accordingly, effects on reaction 1 produced by the addition of these minor amounts of Mn and Ca are expected to be relatively small. Moreover, the extent of this reaction is limited in most orthoamphibolites by the small quantity of kyanite permitted by the bulk composition. Rare gedrite-bearing rocks contain kyanite or partial to complete sillimanite pseudomorphs after kyanite. The aluminosilicate (Als) is in all cases rimmed by cordierite, attesting to its previous equilibrium with orthoamphibole and to lower-temperature and higher-pressure conditions than reaction 1. These coronas are virtually identical to those that occur in the aluminous gneisses discussed below. In addition, we see little evidence remaining for the growth of garnet with cordierite; garnet appears to be replaced by cordierite. Therefore, consumption of garnet and growth of cordierite requires one or more additional reactions. Possible cordierite-producing reactions for these rocks include

$$\text{Grt} + \text{Qz} + \text{H}_2\text{O} = \text{Crd} + \text{Oam} \quad (2)$$

and

$$\text{Grt} + \text{Kspar} + \text{Liq} = \text{Crd} + \text{Bio} \quad (3).$$

Reaction 2 (Qz is quartz) would occur as a continuous reaction as the stable garnet, in the assemblage Grt + Crd + Oam, becomes more iron-rich with falling temperature. However, reaction 2 is limited by the supply of water. Therefore, a reaction involving a melt phase (Liq) such as reaction 3 (Bio is biotite; Kspar is K-feldspar) is more likely because there is other evidence (e.g., Fig. 7) of partial melting having occurred in the Spuhler Peak Metamorphic Suite. Reactions such as (3) could occur with falling temperature (Spear et al., 1999); and fine-grained, low-Ti, green biotite that is commonly present with cordierite may be the result of this reaction.

Orthopyroxene + Cordierite Symplectite

Orthoamphibolite samples containing fine-scale symplectite textures around garnet were collected from a Granite Creek locality (UTM 502873N, 12T 043149E) in the southern Tobacco Roots and from the Leggat Mountain ridge above Quartz Creek (UTM 504011N, 12T 041680E) in the central Tobacco Roots. In the field, these rocks are distinguished by large (2–5 cm),

TABLE 2. CORDIERITE-BEARING ORTHOAMPHIBOLITE

Mineral	Grt core	Grt core	Grt rim	Crd unzoned	Crd unzoned	Ged unzoned	Ged unzoned	Pl core	Pl rim
Oxide (wt%)									
SiO_2	38.81	38.56	38.01	49.14	48.66	48.88	47.63	61.20	59.78
Al_2O_3	21.59	21.43	21.32	32.82	32.49	10.69	10.44	23.90	25.26
TiO_2	0.00	0.00	0.00	0.00	0.00	0.47	0.42	0.00	0.00
MgO	9.53	9.51	5.20	10.83	10.45	18.59	16.89	0.00	0.00
FeO*	26.64	26.80	33.11	5.35	5.27	17.36	19.72	0.00	0.00
MnO	0.72	0.61	1.10	0.00	0.00	0.16	0.28	0.00	0.00
CaO	1.85	2.35	2.02	0.00	0.00	0.41	0.44	5.70	6.83
Na_2O	0.00	0.00	0.00	N.D.	0.58	1.31	1.43	8.13	7.92
K_2O	N.D.†	N.D.	N.D.	N.D.	N.D.	0.00	0.00	0.09	0.08
Total	99.14	99.27	100.75	98.14	97.45	97.87	97.25	99.02	99.86
Elements per Formula									
O	12	12	12	18	18	23	23	8	8
Si	3.01	2.99	3.00	5.00	5.00	6.96	6.93	2.74	2.67
Al	1.97	1.96	1.98	3.94	3.93	1.80	1.79	1.26	1.33
Ti	0.00	0.00	0.00	0.00	0.00	0.05	0.05	0.00	0.00
Mg	1.10	1.10	0.61	1.64	1.60	3.95	3.66	0.00	0.00
Fe	1.73	1.74	2.18	0.46	0.45	2.07	2.40	0.00	0.00
Mn	0.05	0.04	0.07	0.04	0.01	0.02	0.04	0.00	0.00
Ca	0.15	0.20	0.17	N.D.	N.D.	0.06	0.07	0.27	0.33
Na	N.D.	N.D.	N.D.	N.D.	N.D.	0.36	0.40	0.71	0.69
K	N.D.	N.D.	N.D.	N.D.	N.D.	0.00	0.00	0.01	0.01
Total Cations	8.01	8.03	8.02	11.08	10.98	15.27	15.33	4.98	5.01
Mg/(Mg + Fe)	0.39	0.39	0.22	0.78	0.78	0.66	0.60	N.D.	N.D.

Note: Data from Tierney (1994b). Sample: KAT-30, Spuhler Peak Metamorphic Suite (SPMS), UTM 504200N, 12T 041951E. Grt—garnet; Crd—cordierite; Ged—gedrite; Pl—plagioclase.

*FeO—Total iron as FeO.

†N.D.—no data.

Figure 7. Glacially polished outcrop of Spuhler Peak Metamorphic Suite (SPMS) amphibolite showing "wispy" leucosomes consisting principally of plagioclase and quartz. This texture is a common one in the SPMS. Chemically, these outcrops tend to be more iron-rich than amphibolite outcrops with a uniform distribution of mafic and felsic minerals. The hammer in the photo is 40 cm long.

irregularly shaped, pale purple garnet (Grt) porphyroblasts in a coarse (1 cm) matrix of tan gedrite (Ged), quartz (Qz), and biotite (Bio). In thin section, orthopyroxene (Opx), kyanite (Ky), and rutile (Rut) are also clearly part of the coarse equilibrium assemblage. Garnet cores commonly have inclusions of staurolite (Sta) and kyanite (Hatch, 1998b, p. 31), whereas garnet rims have inclusions of the matrix minerals. In several samples, garnet grains are surrounded by a fine-grained, symplectite intergrowth of orthopyroxene and cordierite (Crd). We interpret the coarse-grained assemblage as M1, the symplectite assemblage as M2, and the inclusions in the garnet cores as early M1 or pre-M1.

Symplectite bands 0.2 to 5 mm wide contain wormy, rod-shaped crystals of orthopyroxene that radiate outward from garnet grains in a matrix of cordierite (see Fig. 8). Where present, quartz inclusions in the garnet are also surrounded by the Opx + Crd symplectite. In some cases, a thin band of orthopyroxene directly surrounds quartz grains near garnet. Typical compositions of the minerals in the Opx + Crd symplectite samples are given in Table 3. All of the minerals are chemically homogeneous except for garnet, which is slightly depleted in Mg near the rim. Similar Opx + Crd symplectite textures have been described in rocks from South Africa (Van Reenen, 1986), Antarctica (Harley,

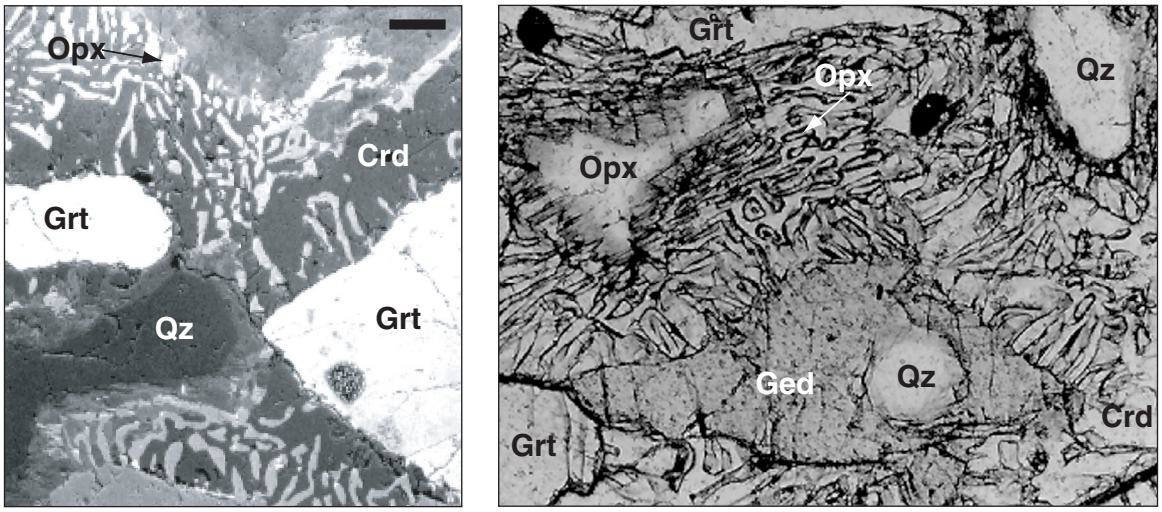

Figure 8. Orthopyroxene (Opx) + cordierite (Crd) symplectite in sample TBR-252H from Granite Creek. On the left is a backscattered electron image (scale bar = 100 μm). On the right is a plane-polarized light photomicrograph (width = 1.5 mm). The symplectite occurs between garnet (Grt) and quartz (Qz), which are never in contact in this sample.

1989), India (Raith et al., 1997), Sri Lanka (Kriegsman and Schumacher, 1999), and elsewhere. These workers and others interpret the symplectite textures to be a result of the reaction

$$\text{Grt} + \text{Qz} = \text{Opx} + \text{Crd} \qquad (4),$$

which is believed (Harley, 1989; Spear, 1993, p. 390) to occur during nearly isothermal decompression at pressures ~0.8 GPa for garnets with the Mg/(Mg + Fe) value (0.5) of those in Table 3 at relatively high temperatures (~700 °C). This texture can also form with cooling or heating as pressure decreases, but the absence of chemical zoning in the symplectite minerals precludes quantitative assessment of the *P-T* path. Hensen and Harley (1990) evaluated experimental data for garnet-orthopyroxene equilibria and calculated isopleths for garnet and orthopyroxene as a function of temperature and pressure. Using the compositions of garnet and orthopyroxene from Table 3, both of Hensen and Harley's (1990) models (their Figures 2.13 and 2.14) yield temperatures of 700 to 770 °C and pressures of 0.75 to 0.9 GPa.

TABLE 3. OPX + CRD SYMPLECTITE

Mineral	Grt core	Grt rim	Crd unzoned	Opx unzoned	Ged unzoned
Oxide (wt%)					
SiO_2	39.90	39.79	50.35	53.23	44.37
Al_2O_3	22.34	22.33	33.77	4.27	18.12
TiO_2	0.00	0.03	0.02	0.07	0.56
MgO	13.45	12.94	12.35	26.21	19.45
FeO*	22.66	22.89	2.01	14.92	11.91
MnO	0.20	0.23	0.03	0.05	0.04
CaO	0.69	0.97	N.D.	0.05	0.27
Na_2O	N.D.†	N.D.	N.D.	N.D.	1.83
K_2O	N.D.	N.D.	N.D.	N.D.	0.02
Total	99.24	99.18	98.53	98.80	96.57
Elements per Formula					
O	12	12	18	6	23
Si	3.01	3.01	5.02	1.93	6.27
Al	1.98	1.99	3.97	0.18	3.02
Ti	0.00	0.00	0.00	0.00	0.06
Mg	1.51	1.46	1.84	1.41	4.10
Fe	1.43	1.45	0.17	0.45	1.41
Mn	0.01	0.01	0.00	0.00	0.01
Ca	0.06	0.08	0.00	0.00	0.04
Na	N.D.	N.D.	0.03	0.00	0.50
K	N.D.	N.D.	N.D.	N.D.	0.00
Total Cations	8.00	8.00	11.02	3.98	15.41
Mg/(Mg+Fe)	0.51	0.50	0.92	0.76	0.74

Note: Data from Hatch (1998a). Sample: TBR-252H, Indian Creek Metamorphic Suite (ICMS), UTM 504011N, 12T 041680E. Grt—garnet; Crd—cordierite; Opx—orthopyroxene; Ged—gedrite.
*FeO—total iron as FeO.
†N.D.—no data.

Sapphirine + Spinel + Cordierite Symplectite

Two orthoamphibolite samples from the Granite Creek locality were observed to have symplectite bands that surround kyanite or sillimanite and separate it from gedrite and biotite. These bands consist of fine-grained intergrowths of elongated sapphirine (Spr) grains and spinel (Spl) in a matrix of cordierite (see Fig. 9). Many of the sapphirine and spinel crystals are aligned roughly perpendicular to the kyanite contact and extend only partway across the band surrounding the aluminosilicate mineral. Sillimanite replaces kyanite in some of these samples. The chemical compositions (Table 4) of the minerals in the Spr + Spl + Crd symplectite sample are very similar to those of the Opx

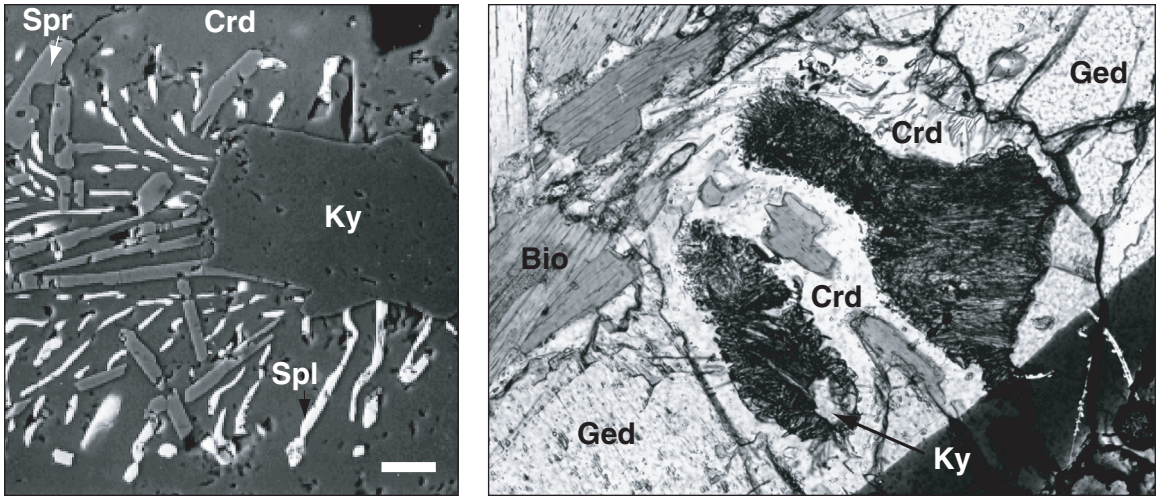

Figure 9. Sapphirine (Spr) + Spinel (Spl) + cordierite (Crd) symplectite in sample CDH-97-51E, also from Granite Creek. On the left is a backscattered electron image (scale bar = 20 μm). On the right is a plane-polarized light photomicrograph (width = 2 mm). The symplectite occurs between kyanite (Ky) and gedrite (Ged) or biotite (Bio).

TABLE 4. SPR + SPL + CRD SYMPLECTITE MINERAL COMPOSITIONS

Mineral	Grt core	Grt rim	Crd unzoned	Opx unzoned	Ged unzoned	Bio unzoned	Spr unzoned	Ky unzoned	Spl normalized
Oxide (wt%)									
SiO_2	40.20	39.97	49.95	53.26	43.93	39.44	12.00	36.84	N.D.
Al_2O_3	22.55	22.31	33.81	3.94	18.15	16.99	64.86	62.63	54.55
TiO_2	0.02	0.04	0.03	0.07	0.63	3.93	0.09	0.03	0.32
MgO	13.84	12.97	12.32	25.71	19.08	18.49	16.46	0.10	9.83
FeO*	22.74	23.44	2.24	16.37	12.43	8.48	5.58	0.21	30.18
MnO	0.23	0.24	0.02	0.07	0.08	0.06	0.01	0.10	2.11
CaO	0.66	0.81	0.01	0.04	0.28	0.07	N.D.	N.D.	N.D.
Na_2O	N.D.†	N.D.	N.D.	N.D.	1.92	0.53	N.D.	N.D.	N.D.
K_2O	N.D.	N.D.	N.D.	N.D.	0.01	7.81	N.D.	N.D.	N.D.
ZnO	N.D.	N.D.	N.D.	N.D.	N.D.	N.D.	N.D.	N.D.	3.01
Total	100.24	99.79	98.37	99.45	96.51	95.79	98.99	99.91	99.99
Elements per Formula									
O	12	12	18	6	23	11	10	5	4
Si	3.00	3.01	5.00	1.93	6.24	2.80	0.71	1.00	N.D.
Al	1.98	1.98	3.99	0.17	3.04	1.42	4.55	2.00	1.83
Ti	0.00	0.00	0.00	0.00	0.07	0.21	0.00	0.00	0.01
Mg	1.54	1.45	1.84	1.39	4.04	1.96	1.46	0.00	0.42
Fe	1.42	1.48	0.19	0.50	1.48	0.50	0.28	0.00	0.72
Mn	0.01	0.02	0.00	0.00	0.01	0.00	0.00	0.00	0.05
Ca	0.05	0.07	0.02	0.00	0.04	0.01	N.D.	N.D.	N.D.
Na	N.D.	N.D.	N.D.	N.D.	0.53	0.07	N.D.	N.D.	N.D.
K	N.D.	N.D.	N.D.	N.D.	N.D.	0.71	N.D.	N.D.	N.D.
Zn	N.D.	N.D.	N.D.	N.D.	N.D.	N.D.	N.D.	N.D.	0.06
Total Cations	8.00	8.00	11.03	3.98	15.44	7.68	7.01	3.01	3.08
Mg/(Mg + Fe)	0.52	0.50	0.91	0.74	0.73	0.80	0.84	N.D.	0.37

Note: Data from Hatch (1998a). Sample: CEH-97-51E, Indian Creek Metamorphic Suite (ICMS), UTM 504011N, 12T 041680E. Spr—sapphirine; Spl—spinel; Crd—cordierite; Grt—garnet; Opx—orthopyroxene; Ged—gedrite; Bio—biotite; Ky—kyanite.

*FeO—total iron as FeO.

†N.D.—no data.

+ Crd symplectite sample (see Table 3). The principal difference seems to be the absence of quartz.

Sapphirine symplectites have been described from many localities (e.g., Lal et al., 1984; Windley et al., 1984; Harley and Hensen, 1990; Kihle and Bucher-Nurminen, 1992; Mohan et al., 1996; Ouzegane and Boumaza, 1996; Godard and Mabit, 1998; Kriegsman and Schumacher, 1999; Elvevold and Gilotti, 2000), but we are not aware of any other occurrences of sapphirine in the Wyoming province. In addition, the details of the Tobacco Root assemblages are not identical to those previously described in the literature. In particular, most sapphirine symplectites in mafic rocks surround sillimanite, rather than kyanite, and occur in amphibole-free rocks that require temperatures higher than the upper stability limit of gedrite (~800 °C). Many involve minerals that are not part of the Tobacco Root assemblages, such as corundum or garnet, or do not have spinel in the symplectite. Descriptions of sapphirine symplectites that do surround kyanite typically are for more felsic rocks with plagioclase as part of the symplectite.

Kihle and Bucher-Nurminen (1992) describe a Spr + Crd symplectite (no spinel) that separates sillimanite and gedrite in feldspar-absent metamorphic rocks from southern Norway, and Windley et al. (1984) describe the same texture from the Limpopo Belt of South Africa. Both papers call for the reaction

$$\text{Ged} + \text{Sil} = \text{Crd} + \text{Spr} \qquad (5).$$

Lal et al. (1984) do have Spr + Spl + Crd symplectites that separate sillimanite and gedrite in rocks they studied from Kiranur, southern India. They suggest the reaction

$$\text{Ged} + \text{Sil} + \text{V} = \text{Crd} + \text{Spr} + \text{Spl} + \text{Ab} \qquad (6)$$

that produces spinel but also feldspar, which is lacking in the Tobacco Root rocks.

The similarities of the Montana Spr + Spl + Crd symplectites to other sapphirine symplectite occurrences, such as the fine grain size, coronal textures, and volume increases, support the interpretation that these features result from decompression reactions. However, it is difficult to balance a reaction with only the minerals in the observed symplectite assemblage, so perhaps one or more important phases are missing. This could be the case if the Spr + Spl + Crd symplectite grew during a decompression melting reaction involving aluminosilicate (Ky or Sil), gedrite, and biotite as the pressure fell from the kyanite to the sillimanite stability field at temperatures between 700 and 800 °C.

Aluminous Gneisses

Garnet-Cordierite-Sillimanite Textures

Aluminous gneisses occur in the Spuhler Peak Metamorphic Suite that typically contain the assemblage quartz + biotite + sillimanite + garnet + plagioclase. The absence of primary (foliation-defining) muscovite and K-feldspar from these rocks is interpreted to be the result of partial melting. In many samples, cordierite + biotite appear to have replaced garnet as a rim and along fractures (Fig. 10). In the same samples, cordierite also appears to be replacing sillimanite. Chemical analyses of the minerals in an aluminous gneiss with cordierite are given in Table 5. These textures might be explained by the continuous reaction

$$\text{Grt} + \text{Sil} + \text{Qz} + \text{H}_2\text{O} = \text{Crd} \qquad (7).$$

As with previously discussed reactions, reaction 7 requires the addition of water if cordierite is hydrous. Alternatively, if a partial melt is present, the reaction

$$\text{Grt} + \text{Kspar} + \text{Liq} = \text{Crd} + \text{Bio} \qquad (3)$$

could produce cordierite and biotite, which commonly occur together in these rocks (Fig. 10). Figure 11 shows a manganese X-ray map of a garnet being replaced by cordierite + biotite. Note the increase in Mn content near the edges of the garnet fragments. We have used the program GIBBS (version 4.7, 2002) of Spear and Menard (1989) to model the chemical variations of garnet being replaced by cordierite by the continuous reaction 7. Figure 12 shows the resulting Mn isopleths (spessartine mole fractions), which are nearly isobaric. Based on this model, measured garnet zoning in the aluminous gneisses

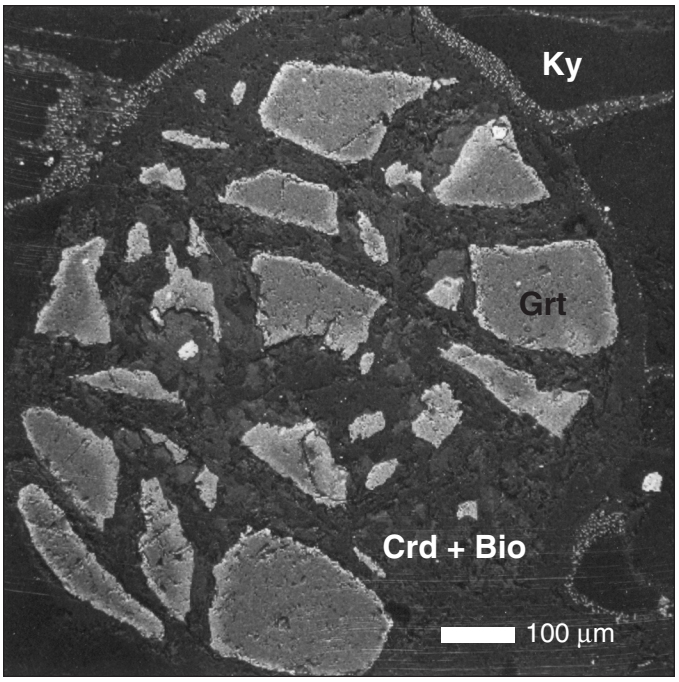

Figure 10. Backscattered electron image of a garnet (Grt) grain being replaced by cordierite (Crd) and biotite (Bio). The thin bright rims on each garnet fragment are manganese-enriched and pyrope-depleted. Sample KAT-41.

TABLE 5. CORDIERITE-BEARING ALUMINOUS GNEISS

Mineral	Grt core	Grt core	Grt rim	Grt rim	Crd unzoned	Crd unzoned	Pl core	Pl rim	Bio core	Bio rim
Oxide (wt%)										
SiO_2	38.20	38.05	36.78	37.89	49.49	49.18	57.49	59.09	37.46	36.74
Al_2O_3	21.14	21.46	20.63	21.03	33.52	33.44	28.21	26.10	17.99	17.97
TiO_2	0.00	0.00	0.00	0.00	0.00	0.00	0.00	0.00	2.07	2.23
MgO	7.26	7.56	3.11	5.95	9.65	8.98	0.00	0.00	14.26	13.86
FeO*	26.68	26.32	26.77	27.03	6.48	6.88	0.00	0.00	14.05	14.49
MnO	4.56	4.56	10.09	6.13	0.84	0.89	0.00	0.00	0.34	0.42
CaO	1.74	1.65	1.51	1.74	N.D.†	N.D.	9.94	7.42	0.00	0.00
Na_2O	N.D.	N.D.	N.D.	N.D.	N.D.	N.D.	6.24	7.66	1.12	0.00
K_2O	N.D.	N.D.	N.D.	N.D.	N.D.	N.D.	0.00	0.09	8.49	8.58
Total	99.58	99.59	98.89	99.77	99.98	99.36	101.88	100.36	94.29	94.29
Elements per Formula										
O	12	12	12	12	18	18	8	8	11	11
Si	3.00	2.99	3.00	3.00	4.98	4.99	2.53	2.63	5.49	5.51
Al	1.96	1.99	1.98	1.96	3.98	4.00	1.47	1.37	3.17	3.12
Ti	0.00	0.00	0.00	0.00	0.00	0.00	0.00	0.00	0.25	0.23
Mg	0.85	0.88	0.38	0.70	1.45	1.36	0.00	0.00	3.09	3.13
Fe	1.75	1.73	1.83	1.79	0.55	0.58	0.00	0.00	1.81	1.73
Mn	0.30	0.30	0.70	0.41	0.07	0.08	0.00	0.00	0.05	0.04
Ca	0.15	0.14	0.13	0.15	N.D.	N.D.	0.47	0.35	0.00	0.00
Na	N.D.	N.D.	N.D.	N.D.	N.D.	N.D.	0.53	0.66	0.00	0.32
K	N.D.	N.D.	N.D.	N.D.	N.D.	N.D.	0.00	0.01	1.64	1.59
Total Cations	8.02	8.02	8.01	8.02	11.03	11.01	5.00	5.02	13.86	14.07
Mg/(Mg + Fe)	0.33	0.34	0.17	0.28	0.73	0.70	N.D.	N.D.	N.D.	0.64

Note: Data from Tierney (1994b). Sample: KAT-42, Spuhler Creek Metamorphic Suite (SPMS), UTM 504188N, 12T 041977E. Grt—garnet; Crd—cordierite; Pl—plagioclase; Bio—biotite.

*FeO—total iron as FeO.

†N.D.—no data.

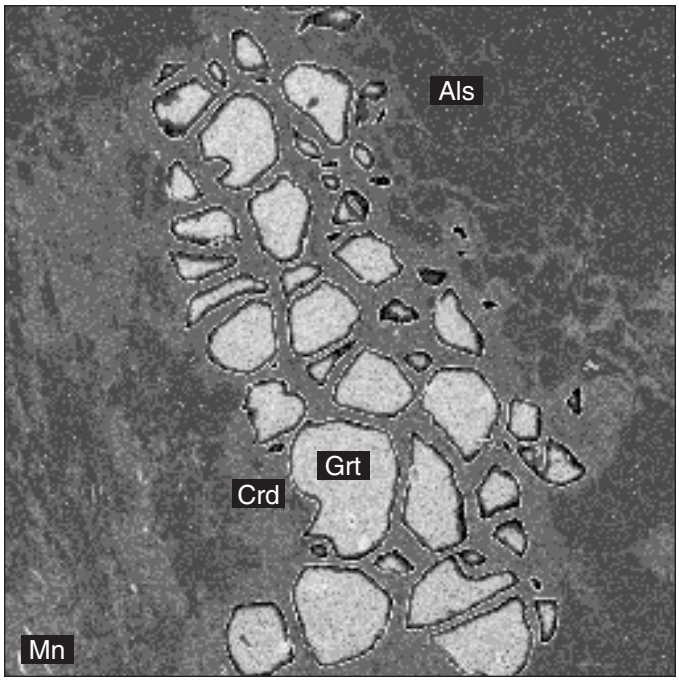

Figure 11. Manganese (Mn) X-ray map for sample KAT-42 showing Mn-enrichment at the rims of garnet (Grt) islands remaining from a single garnet crystal being replaced by cordierite (Crd). The thin "light" rim on each garnet fragment is enriched in Mn, as also shown by the analyses in Table 5. Als—aluminosilicate. Field of view is 5 mm.

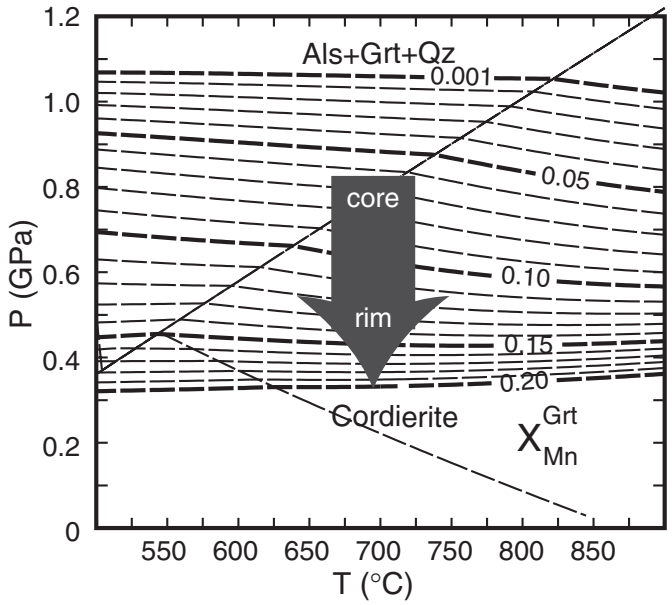

Figure 12. Manganese (Mn) isopleths (mole fraction spessartine) for garnet during the continuous reaction aluminosilicate (Als) + garnet (Grt) + quartz (Qz) = cordierite (Crd) calculated using GIBBS (version 4.7, 2002) of Spear and Menard (1989). The Mn isopleths are virtually parallel to the garnet mode isopleths (not shown) in the MnKFMASH system at constant bulk composition. The large arrow shows the compositional zoning for garnets in cordierite-bearing aluminous gneisses such as KAT-42 in Table 5 at temperatures suggested by geothermometry and other mineral assemblages and textures.

appears to have formed as the pressure fell from 0.8 to 0.4 GPa. The development of the thin Mn-rich rims on the garnet fragments (Fig. 10) is consistent with initial garnet consumption to produce the fragments by crystallizing leucosome via reaction 3 during cooling, followed by a pressure decrease to form the rims on the fragments via reaction 2.

In several aluminous gneiss samples containing kyanite, we observed narrow (20–40 μm) symplectite coronas around both garnet and kyanite (see Figs. 13 and 14). Garnet is rimmed by cordierite and spinel, whereas kyanite is rimmed by anorthite + spinel. The occurrence of these rims on sillimanite pseudomorphs after kyanite as well as on surviving kyanite suggest that these features in both the aluminous gneisses and the orthoamphibolites (discussed above) formed after the sillimanite grew. Because these coronas are surrounded by cordierite in both cases, the coronas may be a fairly late feature caused by the continued breakdown of garnet and kyanite when the supply of other reactants was limited by the surrounding cordierite.

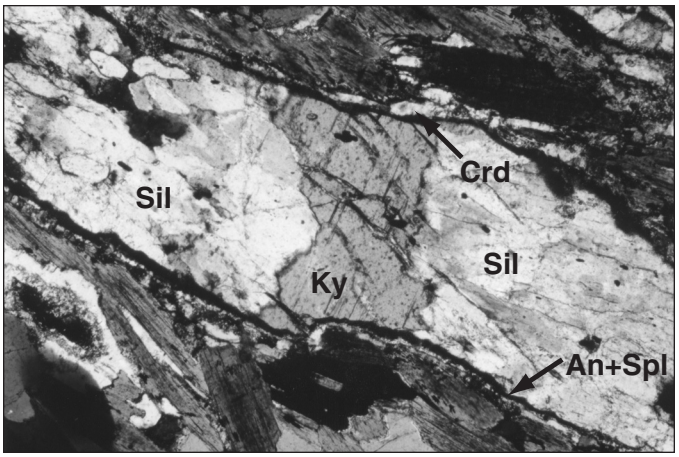

Figure 13. Photomicrograph in cross-polarized light of an anorthite (An) + spinel (Spl) symplectite rim on a sillimanite (Sil) pseudomorph of kyanite (Ky) in sample KAT-41, an aluminous gneiss from the Spuhler Peak Metamorphic Suite. The dark symplectite rim is in turn surrounded by cordierite (Crd). The field of view is 5 mm wide.

Orthopyroxene-Bearing Gneiss

Garnet Necklace Textures

Orthopyroxene-bearing, plagioclase + quartz rocks are locally abundant in the Indian Creek Metamorphic Suite. One distinctive occurrence is on the ridge (UTM 504028N, 12T 041774E) north of Quartz Creek near Leggat Mountain. In this location, mafic aggregates (up to 1 cm across) of orthopyroxene, garnet, and clinopyroxene occur in a plagioclase-quartz matrix. These aggregates are distinguished by orthopyroxene megacrysts (up to 8 mm in diameter) that are separated from the plagioclase-quartz matrix by "necklaces" or coronas of small (0.2 mm), euhedral garnet crystals with associated clinopyroxene, quartz, and hornblende (see Figs. 15 and 16). The orthopyroxene megacrysts have a fractured appearance and contain inclusions of garnet and plagioclase, but not hornblende. Garnet occurs in the plagioclase matrix, as well as in the necklaces and as inclusions in orthopyroxene. Subhedral clinopyroxene and quartz appear to be part of the reaction texture and generally occur on the orthopyroxene side of the necklaces, although quartz also is part of the plagioclase-quartz matrix. Hornblende grains appear to overgrow orthopyroxene near garnet necklaces and contain inclusions of orthopyroxene, clinopyroxene, quartz, and garnet. Ilmenite occurs as an accessory mineral throughout this rock, whereas rutile is found only in the mafic aggregates.

Chemical compositions of the minerals in sample TBR-181c are given in Table 6. The orthopyroxene megacrysts are unzoned. Plagioclase grains in the matrix are nearly homogeneous (An_{49}), with a small anorthite enrichment (An_{52}) at their rims. Plagioclase inclusions in the orthopyroxene are much more albitic (An_{38}) and contain more Fe and Mg. Individual garnets in the matrix have flat compositional profiles with a slight enrichment in grossular and depletion in pyrope at their rims. Necklace garnets have a slight asymmetrical zoning with more grossular on the plagioclase side and more almandine on the orthopyroxene side.

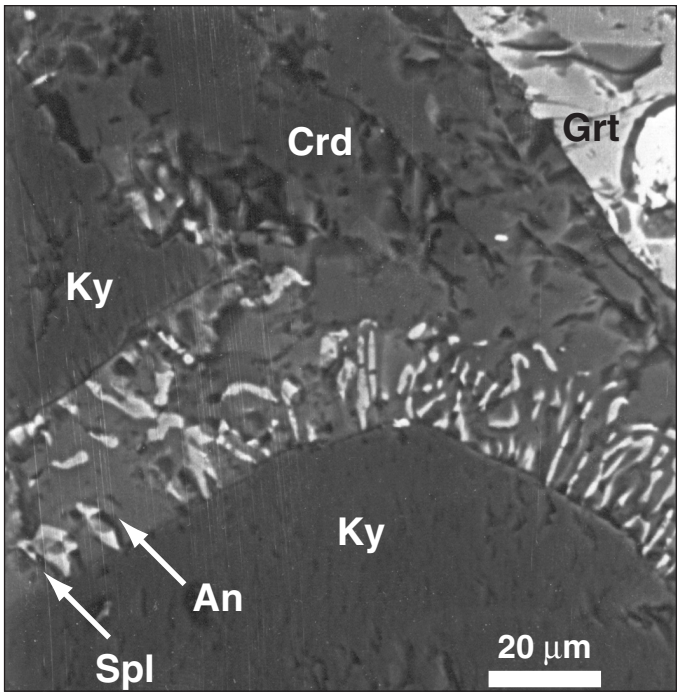

Figure 14. Backscattered electron image of an anorthite (An) + spinel (Spl) symplectite rim on kyanite (Ky) in sample KAT-41, an aluminous gneiss from the Spuhler Peak Metamorphic Suite. The symplectite rim is surrounded by cordierite (Crd).

We interpret the garnet corona texture as a product of a reaction between orthopyroxene and plagioclase (Pl) that occurred as the metamorphic conditions changed from M1 to M2. The corona texture clearly indicates that garnet is a product of the reaction, which led one of us (Tuit, 1996a) initially to argue that

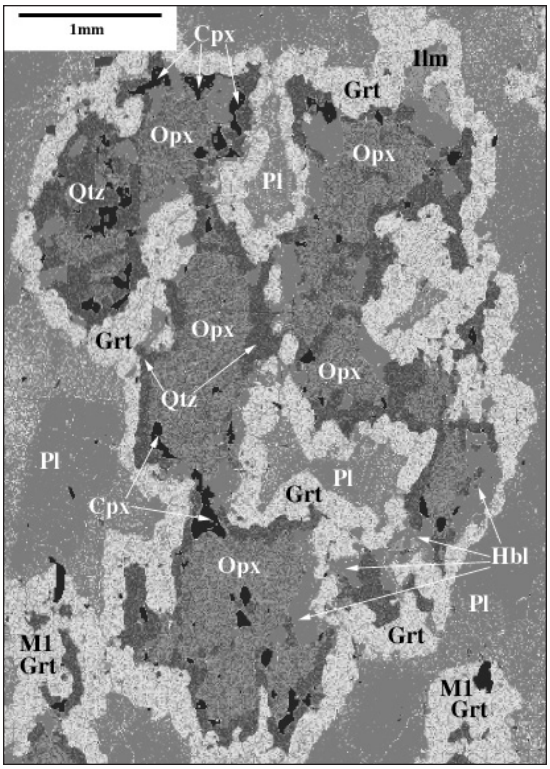

Figure 15. A calcium X-ray map of an orthopyroxene-rich mafic aggregate in a plagioclase-quartz matrix from sample TBR-181c. Lighter shades represent more calcium. Note the calcium-rich garnet bands that separate orthopyroxene from plagioclase.

the reaction was the result of an increase in pressure. However, a decrease in pressure is consistent with other petrologic data, so we believe the garnet-producing reaction

$$\text{Opx} + \text{Pl} = \text{Grt} + \text{Cpx} + \text{Qz} \quad (8)$$

was crossed during falling temperature, rather than rising pressure. Spear and Markussen (1997) studied this reaction in rocks of similar composition and texture from the Adirondack Mountains of New York. They argued for nearly isobaric cooling (−6 bar/°C) based on chemical zoning of minerals and Gibbs method modeling. Minerals in our rocks have similar zoning: Orthopyroxene typically has decreasing Al^{tot} toward the rim; clinopyroxene decreases in Fe/(Fe + Mg) and Al^{tot} and increases in Ca toward the rim; garnet Fe/(Fe + Mg) increases from core to rim. Our samples lack the zoning of Fe/(Fe + Mg) in orthopyroxene and anorthite in plagioclase that Spear and Markussen (1997) observed. The temperature and pressure at which the garnet necklaces were produced depends on composition. For a −6 bar/°C *P-T* cooling path, Spear and Markussen (1997) calculate the following stoichiometry for reaction 8:

$$4\ \text{Opx} + 4\ \text{Pl} = 5\ \text{Grt} + 1\ \text{Cpx} + 1\ \text{Qz} \quad (9).$$

The small modal amounts of clinopyroxene and quartz (relative to garnet) found in the Montana necklaces (Fig. 15) are consistent with the stoichiometry of reaction 9. The garnet necklace texture and its interpretation form an important *P-T* path constraint, especially when contrasted with the garnet pseudomorphs observed in nearby garnet-hornblende amphibolites, as described in the next section.

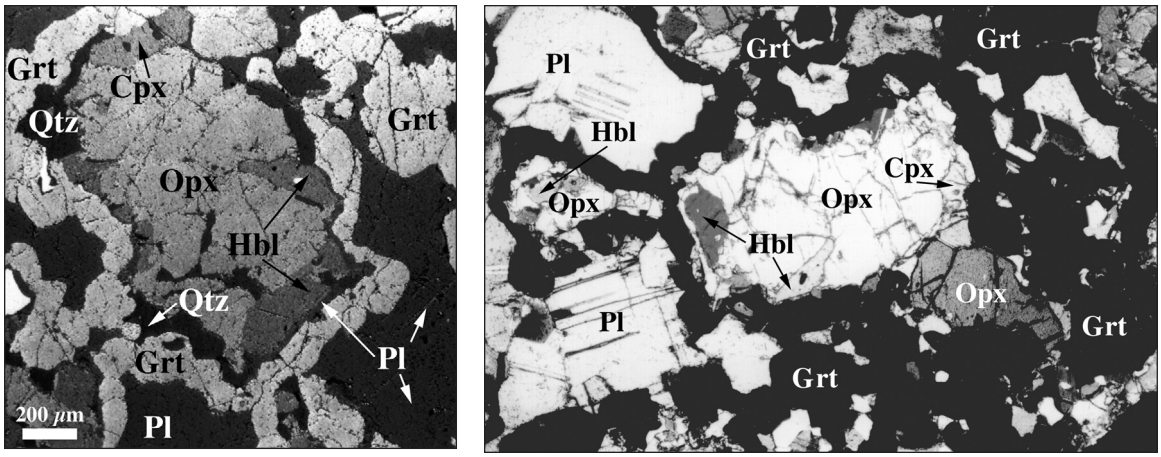

Figure 16. Details of the garnet necklace reaction texture in sample TBR-181c from the Quartz Creek area. On the left is a backscattered electron image (scale bar = 200 μm). On the right is a cross-polarized light photomicrograph (field of view is 4 mm). Bands of polycrystalline garnet with quartz and clinopyroxene separate orthopyroxene and plagioclase. Hornblende growth is believed to postdate the garnet-producing reaction.

TABLE 6. GARNET NECKLACE COMPOSITIONS

Mineral	Grt mafic side	Grt felsic side	Grt mafic side	Grt felsic side	Opx core	Opx rim	Opx core	Opx rim	Cpx core	Cpx rim
Oxide (wt%)										
SiO_2	38.78	38.90	39.27	39.33	54.01	53.51	53.59	52.99	54.66	54.12
Al_2O_3	21.30	21.43	21.83	21.90	1.18	1.10	1.37	1.10	1.60	1.46
TiO_2	N.D.†	N.D.	N.D.	N.D.	0.06	0.09	0.23	0.04	0.31	0.24
MgO	7.07	7.20	7.25	7.24	21.90	21.70	21.62	20.87	14.22	14.26
FeO*	25.17	24.38	25.77	24.30	23.00	23.41	23.94	23.57	7.75	7.58
MnO	0.79	0.56	0.64	0.66	0.20	0.24	0.19	0.19	0.11	0.02
CaO	6.62	7.32	6.77	7.39	0.54	0.45	0.48	0.50	22.36	23.13
Na_2O	N.D.	N.D.	N.D.	N.D.	0.58	0.25	0.30	0.00	0.63	0.41
Total	99.73	99.78	101.54	100.83	101.46	100.74	101.72	99.26	101.64	101.22
Elements per Formula										
O	12	12	12	12	6	6	6	6	6	6
Si	3.01	3.00	2.98	2.99	1.98	1.98	1.97	1.99	1.99	1.98
Al	1.95	1.95	1.95	1.97	0.05	0.05	0.06	0.05	0.07	0.06
Ti	N.D.	N.D.	N.D.	N.D.	0.00	0.00	0.01	0.00	0.01	0.01
Mg	0.82	0.83	0.82	0.82	1.20	1.20	1.18	1.17	0.77	0.78
Fe	1.63	1.58	1.64	1.55	0.71	0.73	0.74	0.74	0.24	0.23
Mn	0.05	0.04	0.04	0.04	0.01	0.01	0.01	0.01	0.00	0.00
Ca	0.55	0.61	0.55	0.60	0.02	0.02	0.02	0.02	0.87	0.91
Na	N.D.	N.D.	N.D.	N.D.	0.04	0.02	0.02	0.00	0.04	0.03
Total Cations	8.00	8.00	7.98	7.97	3.96	4.00	4.00	3.98	3.99	3.99
Mg/(Mg + Fe)	0.33	0.34	0.33	0.35	0.63	0.62	0.62	0.61	0.77	0.77

Mineral	Pl core	Pl rim	Pl core	Pl rim	Pl opx inclu.	Hbl core	Hbl rim	Ilm unzoned	Rut unzoned
Oxide (wt%)									
SiO_2	55.49	54.52	54.96	54.67	55.34	46.74	47.58	N.D.	0.20
Al_2O_3	27.15	27.81	28.82	29.03	24.54	10.18	7.82	N.D.	0.01
TiO_2	0.11	0.08	0.13	0.12	0.11	1.68	1.36	52.48	99.55
MgO	0.11	0.07	0.28	0.40	1.57	13.51	14.82	0.06	N.D.
*FeO	0.08	0.37	0.09	0.32	1.91	10.67	10.11	46.47	0.08
MnO	N.D.	N.D.	N.D.	N.D.	N.D.	0.05	0.07	0.56	0.13
CaO	10.22	10.54	11.14	11.33	7.58	11.72	11.86	N.D.	N.D.
Na_2O	5.94	5.63	5.84	5.17	6.85	1.47	1.01	N.D.	N.D.
K_2O	0.26	0.26	0.25	0.17	0.18	0.69	0.51	N.D.	N.D.
Cr_2O_3	N.D.	N.D.	N.D.	N.D.	N.D.	N.D.	N.D.	N.D.	0.23
Total	99.35	99.29	101.50	101.20	98.07	96.70	95.13	99.56	100.20
Elements per Formula									
O	8	8	8	8	8	23	23	3	2
Si	2.52	2.48	2.45	2.44	2.56	6.82	7.03	N.D.	0.00
Al	1.45	1.49	1.52	1.53	1.34	1.75	1.36	N.D.	0.00
Ti	0.00	0.00	0.00	0.00	0.00	0.18	0.15	1.00	0.99
Mg	0.01	0.00	0.02	0.03	0.11	2.94	3.26	0.00	0.00
Fe	0.00	0.01	0.00	0.01	0.07	1.30	1.25	0.99	0.00
Mn	N.D.	N.D.	N.D.	N.D.	N.D.	0.01	0.01	0.01	0.00
Ca	0.50	0.51	0.53	0.54	0.38	1.83	1.88	N.D.	0.00
Na	0.52	0.50	0.50	0.45	0.61	0.42	0.29	N.D.	0.00
K	0.02	0.02	0.01	0.01	0.01	0.13	0.10	N.D.	0.00
Cr	N.D.	N.D.	N.D.	N.D.	N.D.	N.D.	N.D.	N.D.	0.00
Total Cations	5.02	5.02	5.05	5.02	5.08	15.38	15.32	2.00	1.00
Mg/(Mg + Fe)	N.D.	N.D.	N.D.	N.D.	N.D.	0.69	0.72	N.D.	N.D.

Note: Data from Steiner (1999). Sample: TBR-181c, Indian Creek Metamorphic Suite (ICMS), UTM 504028N, 12T 041774E. Grt—garnet; Opx—orthopyroxene; Cpx—clinopyroxene; Pl—plagioclase; Hbl—hornblende; Ilm—ilmenite; Rut—rutile.

*FeO—total iron as FeO.

†N.D.—no data.

Garnet-Hornblende Amphibolite

Orthopyroxene + Plagioclase Pseudomorphs of Garnet

A few samples of garnet-hornblende amphibolite in the Spuhler Peak Metamorphic Suite contain dodecahedral pseudomorphs after garnet consisting principally of orthopyroxene, plagioclase, and ilmenite (see Fig.17). These pseudomorphs are surrounded by thin coronas of plagioclase + quartz ± orthopyroxene and then hornblende. Very fine needles of cummingtonite may occur in the pseudomorph core and in both the orthopyroxene and the hornblende coronas, although their very fine grain size suggests that their growth may postdate much of the pseudomorphing reaction. Small biotite grains also occur throughout. Quartz is absent from the cores. Spinel and magnetite may be present in the cores. Hornblende is never in contact with garnet. In many cases, some garnet remains in the core. Where remnant garnet is present, plagioclase + orthopyroxene + ilmenite occur along cracks in the garnet as well as surrounding it.

Representative chemical analyses of the minerals in the pseudomorph texture are listed in Table 7. Plagioclase in the core of the pseudomorph is anorthite-rich ($An_{70–85}$), whereas plagioclase in the corona is similar to the matrix plagioclase in composition ($An_{30–45}$). None of the silicate product minerals has Mg/(Mg + Fe) as low as the garnet being replaced, freeing iron to make ilmenite and magnetite.

The consumption of garnet generally requires decreasing pressure or increasing temperature. Because garnet is always separated from hornblende in these rocks, a possible pseudomorphing reaction is

$$Grt + Hbl = Opx + Pl + H_2O \quad (10).$$

Reaction 10 is shown on Figure 18, as part of a series of reactions around a pseudoinvariant point modified from Mukhopadhyay and Bose (1994, Figure 8A therein) and from Pattison (2003, Figure 4B therein) for a rock with Mg/(Mg + Fe) = 0.65 and a_{H_2O} = 0.3. Because of the fine-grained nature of this texture, we think that it is more likely to have developed during decompression than during rising temperature. Other reactions that may be involved are

$$Grt + Qz = Opx + Pl \quad (11)$$

and

$$Grt = Opx + Pl + Spl \quad (12),$$

as suggested by Perkins and Chipera (1985) and Harley (1989). The absence of quartz from the cores implicates the quartz-consuming reaction 11. The presence of spinel suggests the simple garnet breakdown reaction 12. An experimental calibration (Bohlen et al., 1983) of the garnet + quartz reaction 11 is also shown on Figure 18 for the compositions of the minerals given in Table 7. With pressure falling from the ≥1.0 GPa of M1 to the 0.5–0.7 GPa of M2, garnet may have reacted with hornblende (Hbl) and/or quartz and then continued to break down according to reaction 12 as it was separated from the other reactants. Cummingtonite may be produced from orthopyroxene and quartz during falling temperature if water is available. We observed cummingtonite between orthopyroxene and quartz in a texture that is consistent with this reaction (Fig. 19).

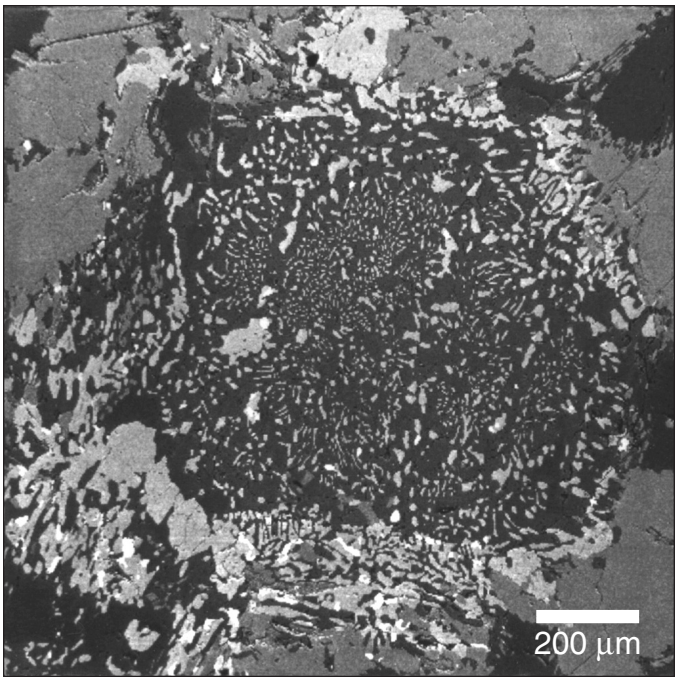

Figure 17. Backscattered electron image of an orthopyroxene + plagioclase pseudomorph of garnet with no relict garnet (sample KAD-10b). The light-colored mineral in the center is orthopyroxene; the dark mineral is plagioclase. The pseudomorph is surrounded by gray hornblende.

The occurrence of garnet necklaces on orthopyroxene in one rock (TBR-181c) within 2 km of another rock (KAD-10b2) with orthopyroxene + plagioclase pseudomorphs of garnet places interesting constraints on the *P-T* path. Because the necklaces occur in the Indian Creek Metamorphic Suite and the pseudomorphs occur in the Spuhler Peak Metamorphic Suite, one might be tempted to conclude that they had a different metamorphic history. However, both textures appear to be late in the metamorphic cycle when other metamorphic and structural evidence supports a common history. The Indian Creek Metamorphic Suite rocks are more magnesian and less calcic, so the garnet necklaces may have developed at higher *T* and *P*. A possible *P-T* path that could have produced these textures is shown in Figure 18. At higher pressure, the reaction

$$Opx + Pl = Grt + Cpx + Qz \quad (8)$$

is crossed as temperature decreases at nearly constant pressure (e.g., −6 bar/°C). When the temperature falls to ~700 °C, the pressure is lowered so that the reaction

TABLE 7. GARNET PSEUDOMORPH ANALYSES

Unit	SPMS	SPMS	SPMS	SPMS	SPMS	SPMS	SPMS	SPMS
Mineral	Grt	Grt	Opx	Opx	Pl	Pl	Cum	Hbl
	core	rim	core	corona	core	rim	corona	matrix
Oxide (wt%)								
SiO_2	37.53	36.67	51.53	52.26	47.84	57.39	55.05	46.04
Al_2O_3	20.44	20.38	1.32	0.55	33.37	27.01	1.09	9.65
TiO_2	0.09	0.03	0.02	0.15	0.02	0.01	0.06	1.23
MgO	4.23	3.27	17.14	18.02	0.09	0.00	18.03	12.33
*FeO	23.62	24.59	27.58	27.72	0.51	0.36	22.16	16.50
MnO	4.65	9.59	1.95	1.07	0.03	0.01	0.97	0.35
CaO	8.30	3.69	0.45	0.48	16.64	9.19	0.64	10.55
Na_2O	†N.D.	N.D.	0.62	0.73	2.37	6.74	0.60	1.78
K_2O	N.D.	N.D.	0.00	0.00	0.01	0.04	0.00	0.35
Total	98.85	98.22	100.60	100.98	100.88	100.74	98.60	98.78
Elements per Formula								
O	12	12	6	6	8	12	23	23
Si	2.99	2.99	1.98	1.99	2.18	2.56	7.93	6.76
Al	1.92	1.96	0.06	0.03	1.79	1.42	0.19	1.67
Ti	0.00	0.00	0.00	0.01	0.00	0.00	0.01	0.14
Mg	0.50	0.40	0.98	1.02	0.01	0.00	3.87	2.70
Fe	1.57	1.68	0.88	0.88	0.02	0.01	2.67	2.03
Mn	0.31	0.66	0.06	0.03	0.00	0.00	0.12	0.04
Ca	0.71	0.32	0.02	0.02	0.81	0.44	0.10	1.66
Na	N.D.	N.D.	0.05	0.05	0.21	0.58	0.17	0.51
K	N.D.	N.D.	0.00	0.00	0.00	0.00	0.00	0.07
Total Cations	8.01	8.01	4.02	4.03	5.03	5.02	15.05	15.56
Mg/(Mg + Fe)	0.24	0.19	0.53	0.54	N.D.	N.D.	0.59	0.57

Note: Data from DeGraff (1996). Sample: KAD-10b2, Spuhler Peak Metamorphic Suite (SPMS), UTM 504200N, 12T 042086E). Grt—garnet; Opx—orthopyroxene; Pl—plagioclase; Cum—cummingtonite; Hbl—hornblende.

*FeO—total iron as FeO.

†N.D.—no data.

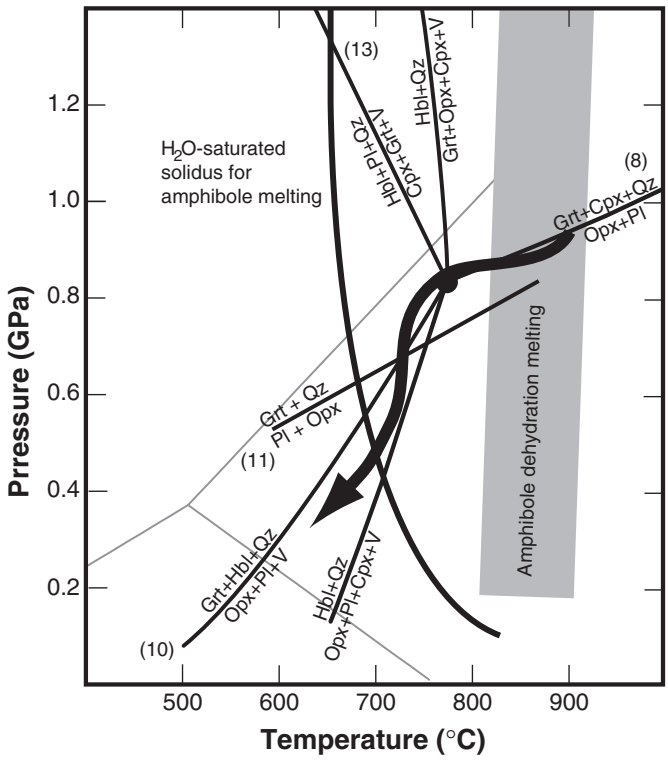

Figure 18. Pressure and temperature estimates for various reactions and a possible *P-T* path (heavy solid line) as discussed in the text. The pseudoinvariant point is based on a bulk composition Mg/(Mg + Fe) value of 0.65, a_{H_2O} of 0.3, and is modified from Figure 8 of Mukhopadhyay and Bose (1994) and Figures 2 and 4B of Pattison (2003). The exact locations of these reaction curves and their intersection are uncertain (see Pattison, 2003), although their relative positions are reasonable and place constraints on the *P-T* path of the Tobacco Root rocks. The curved line is the start of H_2O-saturated melting of amphibole determined by Wolf and Wyllie (1995). The bulk composition–dependent beginning of amphibole dehydration melting is shown as a gray band based Pattison (2003). The single reaction line (11) for the garnet-pseudomorphing reaction garnet (Grt) + quartz (Qz) = plagioclase (Pl) + orthopyroxene (Opx) observed in sample KAD-10b2 is taken from the geobarometer of Bohlen et al. (1983) using the mineral compositions from Table 7 along with a ferric iron correction.

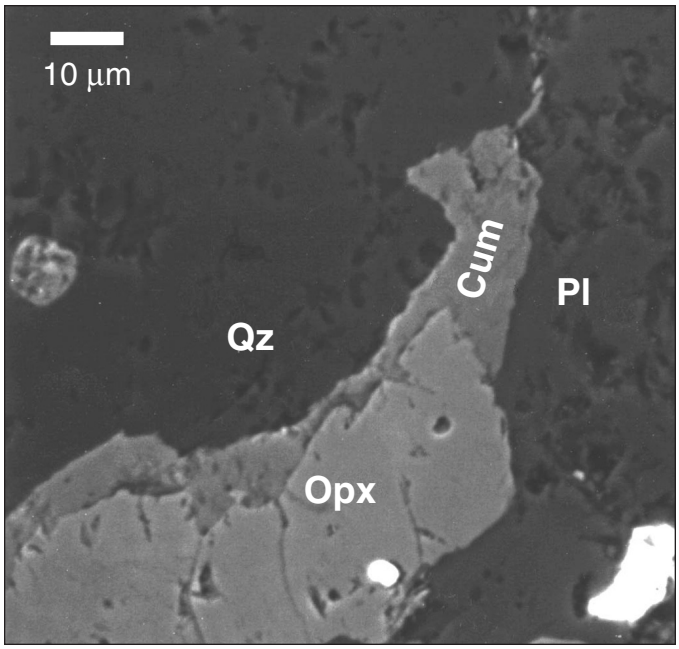

Figure 19. Backscattered electron image of cummingtonite (Cum) separating orthopyroxene (Opx) from quartz (Qz). Sample JB93-50.

$$Grt + Hbl = Opx + Pl + H_2O \quad (10)$$

is crossed at nearly constant temperature. Reactions 11 and 12 may then occur as the pressure is lowered further. If this scenario is correct, nearly isothermal decompression of 0.2 to 0.3 GPa must have occurred late in the Big Sky orogeny.

MMDS Garnet Necklace Texture

A variety of intriguing textures occur in the metamorphosed basalt dikes and sills (MMDS). The MMDS are typically quite fine-grained and granular, with most minerals (plagioclase, clinopyroxene, garnet, hornblende, quartz) 0.1–0.2 mm across. However, they can have a clustered granoblastic texture (Hanley and Vitaliano, 1983) with garnet necklaces separating plagioclase from clinopyroxene and hornblende (Fig. 20). These textures are best preserved in samples that have little foliation. The geometry of the necklaces could be produced by a chemical reaction between plagioclase and clinopyroxene, but the garnet composition (20% grossular, Table 1) does not fall between that of plagioclase and clinopyroxene. A possible explanation is that the rock evolved from a plagioclase-hornblende amphibolite via the reaction

$$Hbl + Pl + Qz = Cpx + Grt + H_2O \quad (13)$$

with the garnet growing next to the plagioclase (the aluminum source) and the clinopyroxene replacing the hornblende. Hornblende was certainly present during garnet growth because it occurs as inclusions in garnet grains. Reaction 13 is included in the amphibolite invariant point shown in Figure 18. To produce the observed texture, the reaction would be crossed as the temperature and pressure rose during the first half of the clockwise *P-T* path. The actual pressure and temperature of this reaction for the MMDS would have been a function of both water activity and the Mg/(Mg + Fe) value for the rock. The presence of hornblende in the rock today would then mean either that the reaction was incomplete or that some of the clinopyroxene has reacted back to hornblende. The fine grain size of the MMDS probably results from the low activity of water and perhaps an absence of melt during metamorphism.

Metapelite and Marble

Metapelites are not particularly common and typically occur as thin units sandwiched between marbles in the Indian Creek Metamorphic Suite. Where pelitic schists do occur, they are commonly graphitic and contain abundant sillimanite (up to 20 mod%) along with garnet, biotite, and quartz ± plagioclase ± orthoclase. The sillimanite occurs both dispersed in the matrix and as blue green bundles that appear to be pseudomorphs after kyanite. In a few samples of Spuhler Peak Metamorphic Suite (Hirst, 1996, p. 43) and Pony–Middle Mountain Metamorphic Suite (Fisher, 1994b, p. 41), K-feldspar occurs in textural equilibrium with kyanite or as inclusions in kyanite. Muscovite is conspicuously absent as a foliation-defining phase, suggesting that muscovite (Mus) dehydration melting has occurred via the reaction

$$Mus + Pl + Qz = Als + Kspar + Melt \quad (14)$$

Garnets may contain inclusions of staurolite and kyanite. We interpret both the staurolite and kyanite as M1. In some Indian

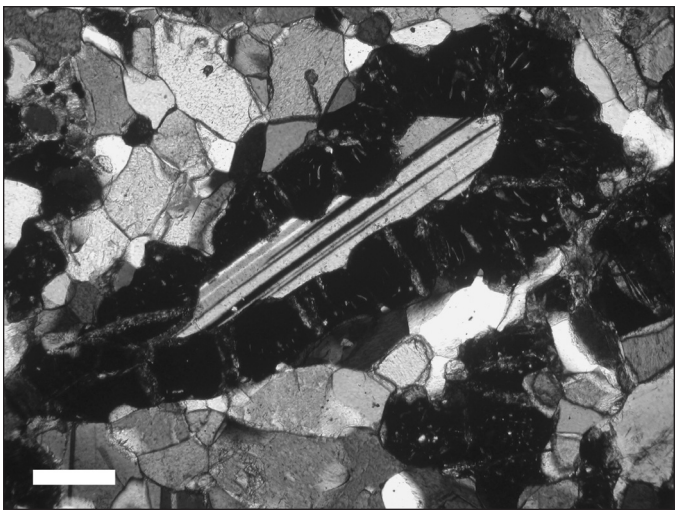

Figure 20. Photomicrograph in cross-polarized light of a metamorphosed basalt dikes and sills sample (SKC-11-2) showing a necklace of garnet grains (extinct) surrounding a single plagioclase grain and separating it from adjacent augite and hornblende grains. Note that the quartz inclusions in the garnets are radial to the plagioclase. Scale bar = 0.2 mm.

Creek Metamorphic Suite rocks only, sillimanite inclusions are found inside garnet indicating that at least some garnet growth occurred in the sillimanite stability field (Fisher, 1994b, Figure 7 therein; Monteleone, 1998a). This sillimanite and the enclosing garnet are possibly remnants from the pre-M1 metamorphism at 2450 Ma (Cheney et al., 2004, this volume, Chapter 8). The occurrence of sillimanite inclusions in garnet requires late garnet growth that normally occurs with increasing temperature in the sillimanite stability field. This raises the possibility of a very different *P-T* path for this older metamorphism, as originally suggested for M1-M2 by Tuit (1996a).

Marble, which best demonstrates the supracrustal origin of the Indian Creek Metamorphic Suite, also contains evidence of at least two episodes of metamorphism. In some samples, the high-grade assemblage calcite + diopside + forsterite can be observed, although the forsterite is commonly replaced partially by serpentine. Nearby, quartz pods and quartzite layers in the marble are typically rimmed by tremolite, which also occurs as coarse (2–4 cm), randomly oriented blades in the calcite + dolomite marble.

PRESSURE-TEMPERATURE-TIME EVOLUTION OF THE TOBACCO ROOT MOUNTAINS

The mineralogy, texture, and chemistry of the metamorphic rocks of the Tobacco Root Mountains can be used to document a fairly detailed pressure-temperature-time (*P-T*-t) history for the northwestern edge of the Wyoming province. This metamorphic history began (M0) near the start of the Proterozoic era at 2.45 Ga (see Cheney et al., 2004, this volume, Chapter 8) with a high-grade metamorphic event (Reid [1963] metamorphism *a*, Vitaliano et al. [1979] M1). This first metamorphism produced coarse (cm-scale) gneissic banding in many rocks and may have led to partial melting. Some of the minerals in the rocks today may have grown during M0, but in most cases it is not possible to prove that they did not grow or recrystallize during a subsequent metamorphism (M1 or M2). The rocks were cooled enough following M0 to permit the intrusion of basaltic dikes (MMDS) at high angles to foliation and to produce chilled margins in the dikes (Brady et al., 2004b, this volume, Chapter 7). Although these dikes, dated at 2.07 Ga (Mueller et al., 2004, this volume, Chapter 9), occur throughout the Tobacco Root Mountains and in the adjacent Highland Range, they do not intrude the Spuhler Peak Metamorphic Suite. In addition, there is no evidence of monazite or zircon growth in the Spuhler Peak Metamorphic Suite at 2.45 Ga (Cheney et al., 2004, this volume, Chapter 8; Mueller et al., 2004, this volume, Chapter 9), so we believe that all the metamorphic features of the Spuhler Peak Metamorphic Suite and the MMDS were produced during the Big Sky orogeny at 1.77 Ga.

All of the metamorphic rock suites in the Tobacco Roots have at least some samples that have both higher-pressure and lower-pressure mineral assemblages. Large (cm-scale) porphyroblasts of minerals such as kyanite, orthopyroxene, clinopyroxene, orthoamphibole, and garnet define a texture that is overprinted by later, fine-grained minerals such as sillimanite, cordierite, sapphirine, orthopyroxene, hornblende, biotite, and cummingtonite. We believe that these two textures (assigned to M1 and M2, respectively) developed during a single metamorphism at 1.77 Ga along a clockwise *P-T* path (Fig. 21). Although the actual *P-T* path for different areas in the Tobacco Root Mountains may deviate from the proposed summary path, many of the features used to define the path can be found across the range.

Large garnet crystals in the Indian Creek Metamorphic Suite contain staurolite and kyanite inclusions, although staurolite does not occur as a matrix mineral. Thus, the metamorphic record begins in the staurolite-kyanite zone. The upper stability limit of staurolite (Spear, 1993) is shown on Figure 21. Rocks of the Indian Creek Metamorphic Suite contain coarse orthopyroxene and kyanite in the same thin section, which we believe (Fig. 4) is evidence for pressures above 1.0 GPa and temperatures over 700 °C. We also observed Kspar inclusions in large kyanite crystals of the Spuhler Peak Metamorphic Suite, which are consistent with a minimum pressure of 0.8 GPa and a minimum temperature of 700 °C (Spear et al., 1999). The coarse grain size of the high-pressure assemblages (Fig. 5), migmatitic field relations (Fig. 7), and the virtual absence of muscovite from aluminous rocks are all consistent with partial melting during metamorphism. Recognizing that the amount of melting depends on many factors but particularly on the bulk composition of even specific protoliths, an amphibolite minimum melting curve (Wolf and Wyllie, 1995) is placed on Figure 21 for reference. In high-grade metamorphic terranes, melts will form once the temperature exceeds that of the water-saturated melting curve. The amount of this water-saturated melt will be small as it is controlled by the vanishingly small amount of water in such rocks (Spear et al., 1999). At temperatures greater than the water-saturated melting temperature for each rock composition, all dehydration reactions are melting reactions. The occurrence of abundant biotite in many bulk compositions, and the lack of orthopyroxene + K-feldspar or orthopyroxene-bearing migmatites limits the maximum temperature to 850 °C at ~0.7 GPa, as shown on Figure 4 and also on Figure 21. The partial to complete sillimanite pseudomorphs after kyanite that occur in garnet + orthoamphibole rocks from the Spuhler Peak Metamorphic Suite require that the *P-T* path pass to the low-temperature side of the invariant point on Figure 4. Similarly, the abundance of orthoamphibole in the Spuhler Peak and Indian Creek Metamorphic Suites limits the *P-T* path of most samples to temperatures below the upper stability of orthoamphibole (Fig. 4).

Garnet necklaces (~300 μm across, Fig.15) surround orthopyroxene crystals in Opx + Pl gneisses. Their coronal texture and size is believed to result from nearly isobaric cooling at ~0.8 GPa. Nearby, Opx + Pl pseudomorphs of garnet in hornblende amphibolites (Fig. 17; Table 7) appear to record nearly isobaric decompression. The juxtaposition of these two textures can be explained by an abrupt change in *P-T* trajectory (Fig. 21) that is consistent with other minerals and textures. For example, fine-grained pseudomorphs and symplectite reaction textures developed in a number of rocks during decompression at high temperatures. Orthopyroxene + cordierite symplectites rimming

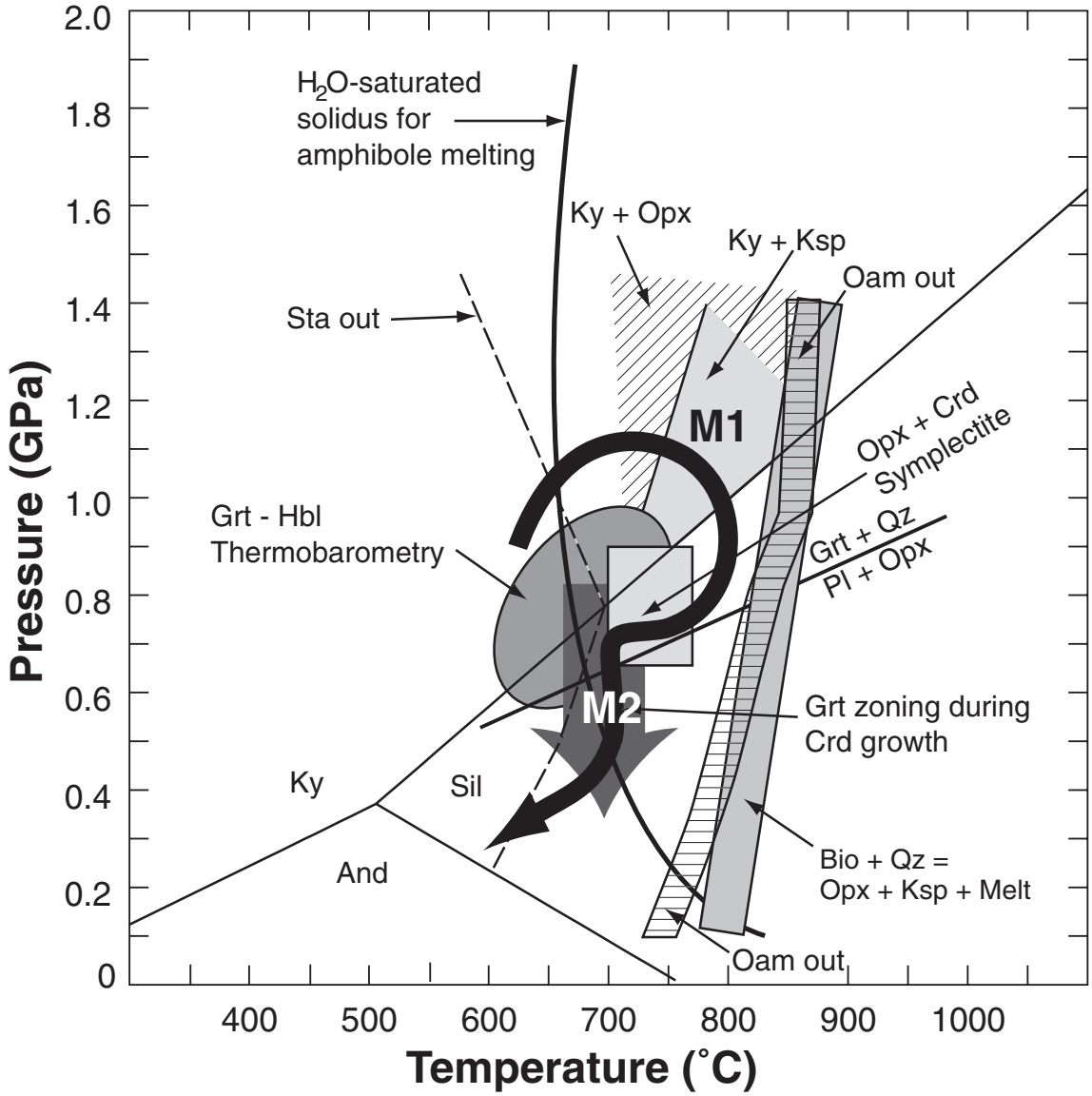

Figure 21. Summary diagram showing constraints on the pressure-temperature evolution of the metamorphic rocks of the Tobacco Root Mountains as outlined in this paper. Specific fields outlined on the diagram are (1) the temperatures and pressures (dashed line) above which staurolite is no longer stable (Spear, 1993), (2) a dehydration melting curve for amphibolite (Fig. 18), (3) the lower part (triangular region) of the stability field of kyanite + orthopyroxene (Fig. 4), (4) the temperatures and pressures (line with hatch marks) above which orthoamphibole is no longer stable (Fig. 4), (5) the lower part (triangular region) of the stability field of kyanite + K-feldspar resulting from dehydration melting (Spear et al., 1999), (6) the range of temperatures and pressures (dark oval) calculated from the garnet-hornblende-plagioclase-quartz thermobarometer (Fig. 2), (7) garnet-orthopyroxene equilibria field (rectangular box) for the orthopyroxene + cordierite symplectite of Table 3 (Hensen and Harley, 1990), (8) the calculated location (solid line) of the garnet pseudomorphing reaction garnet + quartz = plagioclase + orthopyroxene (Fig. 18), (9) the dehydration melting of biotite + quartz provides a maximum temperature as there are no orthopyroxene + K-feldspar rocks in the Tobacco Root Mountains, and (10) a calculated decompression path (wide arrow) resulting from cordierite growth based on observed Mn zoning of garnet (Fig. 12). A possible *P-T* path based on these constraints for the 1.77 Ga Big Sky orogeny is shown by the heavy black line. To produce both the garnet necklaces on orthopyroxene and the orthopyroxene + plagioclase pseudomorphs of garnet in nearby rocks, a nearly isobaric cooling at high pressure must be followed by a nearly isothermal decompression. We believe these and other features are related to tectonic unroofing during extension late in the metamorphic cycle. Sta—staurolite; And—andalusite.

garnet in Indian Creek Metamorphic Suite samples (Fig. 8; Table 3) developed at 700–770 °C and 0.75–0.9 GPa, according to the calculations of Hensen and Harley (1990). Chemical zoning of Mn in garnet grains (Figs. 10 and 11; Table 2) being pseudomorphed by cordierite is consistent with pressure falling from 0.8 to 0.5 GPa at high temperature (Fig. 12). A large proportion of the mafic samples studied are decorated with extremely fine-grained, needlelike sprays of cummingtonite that may have grown upon fairly rapid decompression, followed by fairly rapid cooling.

The high pressures and temperatures recorded in Tobacco Root metamorphic rocks require deep burial in a continental-scale collision. Clearly, the Big Sky orogeny matches other Himalayan-scale events. And like some other large orogenies, we see abundant evidence for significant decompression at high temperatures (Spear, 1993, Chapter 21 therein). Reaction constraints involving garnet and orthopyroxene (Fig. 18) make tectonic denudation the likely cause for this decompression, both for the observed metamorphic textures and for the subsequent rapid cooling leading to similar radiometric ages for zircon, monazite, hornblende and biotite (Brady et al., 2004a, this volume, Chapter 5; Cheney et al., 2004, this volume, Chapter 8; Mueller et al., 2004, this volume, Chapter 9).

ACKNOWLEDGMENTS

The authors thank the W.M. Keck Foundation and the colleges that form the Keck Geology Consortium for the support of this work over many years. We also thank the many faculty members at those colleges who advised the undergraduate theses that form the basis for our results. We appreciate very much the thoughtful reviews of the manuscript by John C. Schumacher and Frank S. Spear.

REFERENCES CITED

Archuleta, L.L., 1994a, The mineralogy and petrology of garnet-amphibole rocks from the Spuhler Peak Formation along Thompson Peak ridge, Tobacco Root Mountains, SW Montana, *in* Wilson, M.A., ed., Seventh Keck research symposium in geology: San Antonio, Texas, p. 60–63.

Archuleta, L.L., 1994b, Mineralogy, petrography, and geochemistry including geothermobarometry of an aluminous enclave rock and host rocks within the Spuhler Peak Formation, Tobacco Root Mountains, southwestern Montana [B.A. thesis]: Claremont, California, Pomona College, 75 p.

Bohlen, S.R., Wall, V.J., and Boettcher, A.L., 1983, Experimental investigations and geological applications of equilibria in the system FeO-TiO_2-Al_2O_3-SiO_2-H_2O: American Mineralogist, v. 68, p. 1049–1058.

Brady, J.B., Carmichael, S., Burger, H.R., Harris, C., Cheney, J.T., and Harms, T.A., 1998a, Thermobarometry and geochemistry of metamorphosed mafic dikes and sills (MMDS) of the Tobacco Root Mountains, Montana: Geological Society of America Abstracts with Programs, v. 30, no. 7, p. 97.

Brady, J.B., Cheney, J.T., Rhodes, A.L., Vasquez, A., Green, C., Duvall, M., Kogut, A., Kaufman, L., and Kovaric, D., 1998b, Isotope geochemistry of Proterozoic talc occurrences in Archean marbles of the Ruby Mountains, southwest Montana, USA: Geological Materials Research, v. 2, p. 41.

Brady, J.B., Kovaric, D.N., Cheney, J.T., Jacob, L.J., and King, J.T., 2004a, $^{40}Ar/^{39}Ar$ ages of metamorphic rocks from the Tobacco Root Mountains region, Montana, *in* Brady, J.B., et al., eds., Precambrian geology of the Tobacco Root Mountains, Montana: Boulder, Colorado, Geological Society of America Special Paper 377, p. 131–149 (this volume).

Brady, J.B., Mohlman, H.K., Harris, C., Carmichael, S.K., Jacob, L.K., and Chaparro, W.R., 2004b, General geology and geochemistry of metamorphosed Proterozoic mafic dikes and sills, Tobacco Root Mountains, Montana, *in* Brady, J.B., et al., eds., Precambrian geology of the Tobacco Root Mountains, Montana: Boulder, Colorado, Geological Society of America Special Paper 377, p. 89–104 (this volume).

Burger, H.R., 1966, Structure, petrology, and economic geology of the Sheridan District, Madison County, Montana [Ph.D. thesis]: Bloomington, Indiana University, 156 p.

Burger, H.R., 1969, Structural evolution of the southwestern Tobacco Root Mountains, Montana: Geological Society of America Bulletin, v. 80, p. 1329–1341.

Burger, H.R., 2004, General geology and tectonic setting of the Tobacco Root Mountains, Montana, *in* Brady, J.B., et al., eds., Precambrian geology of the Tobacco Root Mountains, Montana: Boulder, Colorado, Geological Society of America Special Paper 377, p. 1–14 (this volume).

Burger, H.R., Peck, W.H., Johnson, K.E., Tierney, K.A., Poulsen, C.J., Cady, P., Lowell, J., MacFarlane, W.A., Sincock, M.J., Archuleta, L.L., Pufall, A., and Cox, M.J., 2004, Geology and geochemistry of the Spuhler Peak Metamorphic Suite, *in* Brady, J.B., et al., eds., Precambrian geology of the Tobacco Root Mountains, Montana: Boulder, Colorado, Geological Society of America Special Paper 377, p. 47–70 (this volume).

Cady, P., 1994a, Petrographic analysis of amphibolites from the Spuhler Peak Formation, Indian Creek Metamorphic Suite, and Pony–Middle Mountain Metamorphic Complex, Tobacco Root Mountains, Montana, *in* Wilson, M.A., ed., Seventh Keck research symposium in geology: San Antonio, Texas, p. 64–66.

Cady, P., 1994b, Petrographic and geochemical analysis of amphibolites from the Tobacco Root Mountains, Montana [B.A. thesis]: Colorado Springs, Colorado College, 86 p.

Carmichael, S.K., 1998a, Geothermobarometry of metamorphosed mafic dikes and sills, Tobacco Root Mountains, southwestern Montana, *in* Mendelson, C.V., and Mankiewicz, C., eds., Eleventh Keck research symposium in Geology: Amherst, Massachusetts, Amherst College, p. 168–171.

Carmichael, S.K., 1998b, Geothermobarometry of metamorphosed mafic dikes and sills, Tobacco Root Mountains, southwestern Montana [B.A. thesis]: Northampton, Massachusetts, Smith College, 51 p.

Carmichael, S.K., Brady, J.B., Cheney, J.T., and Mohlman, H.K., 1998, Metamorphic history of mafic dikes and sills in the Tobacco Root Mountains, southwestern Montana: Geological Society of America Abstracts with Programs, v. 30, no. 1, p. 10.

Carrington, D.P., and Harley, S.L., 1995, Partial melting and phase relations in high-grade metapelites; an experimental petrogenetic grid in the KFMASH system: Contributions to Mineralogy and Petrology, v. 120, no. 3–4, p. 270–291.

Cheney, J.T., Brady, J.B., Burger, H.R., Fisher, R., Jacob, L., King, J.T., Tierney, K.A., Peck, W.H., Poulsen, C.J., Cady, P., Lowell, J., Sincock, M.J., and Archuleta, L.L., 1994, Metamorphic evolution of Archean rocks in the Tobacco Root Mountains of SW Montana: Geological Society of America Abstracts with Programs, v. 26, no. 7, p. 226.

Cheney, J.T., Brady, J.B., Burger, H.R., Harms, T.A., Johnson, K.E., DeGraff, K.A., King, J.F., Mohlman, H.K., Tuit, C.B., Hirst, J., and Wegmann, K.W., 1996, Tectonometamorphic evolution of Archean amphibolites from the Tobacco Root Mountains of Montana: Geological Society of America Abstracts with Programs, v. 28, no. 7, p. 45.

Cheney, J.T., Hatch, C.E., Harms, T.A., Brady, J.B., Burger, H.R., and Monteleone, B.D., 1998, Sapphirine symplectite bearing kyanite-orthopyroxene orthoamphibolite from the Archean Indian Creek Metamorphic Suite (ICMS), Tobacco Root Mountains, Montana: Geological Society of America Abstracts with Programs, v. 30, no. 7, p. 97.

Cheney, J.T., Webb, A.A.G., Coath, C.D., and McKeegan, K.D., 2004, In situ ion microprobe $^{207}Pb/^{206}Pb$ dating of monazite from Precambrian metamorphic suites, Tobacco Root Mountains, Montana, *in* Brady, J.B., et al., eds., Precambrian geology of the Tobacco Root Mountains, Montana: Boulder, Colorado, Geological Society of America Special Paper 377, p. 151–179 (this volume).

Cordua, W.S., 1973, Precambrian geology of the southern Tobacco Root Mountains, Madison County, Montana [Ph.D. thesis]: Bloomington, Indiana University, 247 p.

DeGraff, K., 1996a, Petrology of amphibolites from the Archean Spuhler Peak Metamorphic Suite of the Tobacco Root Mountains, SW Montana [B.A. thesis]: Amherst, Massachusetts, Amherst College, 74 p.

DeGraff, K., 1996b, Petrology of amphibolites from the Archean Spuhler Peak metamorphic suite of the Tobacco Root Mountains, southwestern

Montana, *in* Mendelson, C.V., and Mankiewicz, C., eds., Ninth Keck research symposium in geology: Williamstown, Massachusetts, Williams College, p. 94–97.

DeGraff, K.A., Tierney, K.A., Cheney, J.T., and Brady, J.B., 1996, Petrology of amphibolites from the Archean Spuhler Peak metamorphic suite (SPMS) of the Tobacco Root Mountains, Montana: Geological Society of America Abstracts with Programs, v. 28, no. 3, p. 48.

Elvevold, S., and Gilotti, J.A., 2000, Pressure-temperature evolution of retrogressed kyanite eclogites, Weinschenk Island, Northeast Greenland Caledonides: Lithos, v. 53, no. 2, p. 127–147.

Fisher, R., 1994a, Deducing metamorphic histories first step: Garnet zoning in metapelites, *in* Wilson, M.A., ed., Seventh Keck research symposium in geology: San Antonio, Texas, p. 67–70.

Fisher, R.G.M., 1994b, Comparative metamorphic histories of three high-grade gneiss terrains in the Tobacco Root Mountains of southwest Montana [B.A. thesis]: Northampton, Massachusetts, Smith College, 69 p.

Friberg, N., 1976, Petrology of a metamorphic sequence of upper-amphibolite facies in the central Tobacco Root Mountains, southwestern Montana [Ph.D. thesis]: Bloomington, Indiana University, 146 p.

Friberg, L.M., 1994, Geothermobarometry of Precambrian metamorphic rocks from the Tobacco Root Mountains of southwestern Montana: Geological Society of America Abstracts with Programs, v. 26, no. 5, p. 16.

Frisch, J.D., 1998a, Geothermobarometry of garnet amphibolites from the Indian Creek and Pony–Middle Mountain metamorphic suites, Tobacco Root Mountains, Montana, *in* Mendelson, C.V., and Mankiewicz, C., eds., Eleventh Keck research symposium in Geology: Amherst, Massachusetts, Amherst College, p. 172–175.

Frisch, J.D., 1998b, Geothermobarometry of Garnet-Amphibolites form the Indian Creek and Pony Middle Mountain Metamorph8ic Suites, Tobacco Root Mountains, Montana [B.A. thesis]: Amherst, Massachusetts, Amherst College, 85 p.

Frisch, J.D., and Cheney, J.T., 1998, Geothermobarometry of garnet-amphibolites from the Indian Creek and Pony–Middle Mountain metamorphic suites, Tobacco Root Mountains, Montana: Geological Society of America Abstracts with Programs, v. 30, no. 1, p. 20.

Gillmeister, N.M., 1972a, Cherry Creek Group–Pony Group relationship in the central Tobacco Root Mountains, Madison County, Montana: Northwest Geology, v. 1, p. 21–24.

Gillmeister, N.M., 1972b, Petrology of Precambrian rocks in the central Tobacco Root Mountain, Madison County, Montana: Cambridge, Massachusetts, Harvard University, Cambridge, 201 p.

Godard, G., and Mabit, J.-L., 1998, Peraluminous sapphirine formed during retrogression of a kyanite-bearing eclogite from Pays de Leon, Armorican Massif, France: Lithos, v. 43, no. 1, p. 15–29.

Graham, C.M., and Powell, R., 1984, A garnet-hornblende geothermometer; calibration, testing, and application to the Pelona Schist, southern California: Journal of Metamorphic Geology, v. 2, no. 1, p. 13–31.

Hanley, T.B., 1975, Structure and petrology of the northwestern Tobacco Root Mountains, Madison County, Montana [Ph.D. thesis]: Bloomington, Indiana University, 289 p.

Hanley, T.B., 1976, Stratigraphy and structure of the Central Fault Block, northwestern Tobacco Root Mountains, Madison County, Montana, *in* Anonymous, ed., Guidebook, The Tobacco Root Geological Society 1976 Field Conference: Butte, Montana, Montana Bureau of Mines and Geology Special Publication 73, p. 7–14.

Hanley, T.B., and Vitaliano, C.J., 1983, Petrography of Archean mafic dikes of the Tobacco Root Mountains, Madison County, Montana: Northwest Geology, v. 12, p. 43–55.

Harley, S.L., 1985, Paragenetic and mineral-chemical relationships in orthoamphibole-bearing gneisses from Enderby Land, East Antarctica; a record of Proterozoic uplift: Journal of Metamorphic Geology, v. 3, no. 2, p. 179–200.

Harley, S.L., 1989, The origins of granulites: A metamorphic perspective: Geological Magazine, v. 126, p. 215–247.

Harley, S.L., and Hensen, B.J., 1990, Archaean and Proterozoic high-grade terranes of East Antarctica (40–80 degrees E); a case study of diversity in granulite facies metamorphism, *in* Ashworth, J.R., and Brown, M., eds., High-temperature metamorphism and crustal anatexis: The Mineralogical Society Series 2, p. 320–370.

Hatch, C.E., 1998a, Sapphirine symplectites in orthoamphibolites of the Archean Indian Creek metamorphic suite (ICMS), Tobacco Root Mountains, Montana, *in* Mendelson, C.V., and Mankiewicz, C., eds., Eleventh Keck research symposium in Geology: Amherst, Massachusetts, Amherst College, p. 180–183.

Hatch, C.E., 1998b, Sapphirine symplectities in orthoamphibole gneiss of the Archean Indian Creek Metamorphic Suite, Tobacco Root Mountains, Montana [B.A. thesis]: Amherst, Massachusetts, Amherst College, 110 p.

Hatch, C.E., and Cheney, J.T., 1998, Geothermobarometry in the Archean Indian Creek Metamorphic Suite (ICMS) rocks in the Tobacco Root Mountains, Montana: Geological Society of America Abstracts with Programs, v. 30, no. 1, p. 24.

Hensen, B.J., and Harley, S.L., 1990, Graphical analysis of P-T-X relations in granulite facies metapelites, *in* Ashworth, J.R., and Brown, M., eds., High-temperature metamorphism and crustal anatexis: The Mineralogical Society Series 2, p. 19–56.

Hess, D.F., 1967, Geology of pre-Beltian rocks in the central and southern Tobacco Root Mountains (Montana), with reference to superposed effects of the Laramide age Tobacco Root Batholith [Ph.D. thesis]: Bloomington, Indiana University, 333 p.

Hess, D.F., and Vitaliano, C.J., 1990, Metabasites; an indicator of Late Archean geologic history in the Tobacco Root Mountains, Madison County, Montana: Geological Society of America Abstracts with Programs, v. 22, no. 5, p. 13.

Hirst, J., 1996, Mineralogy, petrology, and geothermobarometry of aluminous Archean rocks in the Spuhler Peak metamorphic suite of the Tobacco Root Mountains, southwestern Montana [B.A. thesis]: Claremont, California, Pomona College, 64 p.

Hodges, K.V., and Spear, F.S., 1982, Geothermometry, geobarometry and the Al_2SiO_5 triple point at Mt. Moosilauke, New Hampshire: American Mineralogist, v. 67, no. 11–12, p. 1118–1134.

Holdaway, M.J., 1971, Stability of andalusite and the aluminum silicate phase diagram: American Journal of Science, v. 271, p. 97–131.

Holland, T.J.B., and Powell, R., 1998, An internally consistent thermodynamic data set for phases of petrological interest: Journal of Metamorphic Geology, v. 16, no. 3, p. 309–343.

Immega, I.P., and Klein, C., Jr., 1976, Mineralogy and petrology of some metamorphic Precambrian iron-formations in southwestern Montana: American Mineralogist, v. 61, no. 11–12, p. 1117–1144.

Johnson, K.E., Brady, J.B., MacFarlane, W.A., Thomas, R.B., Poulsen, C., and Sincock, M.J., 2004, Precambrian meta-ultramafic rocks from the Tobacco Root Mountains, Montana, *in* Brady, J.B., et al., eds., Precambrian geology of the Tobacco Root Mountains, Montana: Boulder, Colorado, Geological Society of America Special Paper 377, p. 71–87 (this volume).

Kihle, J., and Bucher-Nurminen, K., 1992, Orthopyroxene-sillimanite-sapphirine granulites from the Bamble granulite terrane, southern Norway: Journal of Metamorphic Geology, v. 10, no. 5, p. 671–683.

Kohn, M.J., and Spear, F.S., 1990, Two new geobarometers for garnet amphibolites, with applications to southeastern Vermont: American Mineralogist, v. 75, no. 1–2, p. 89–96.

Kriegsman, L.M., and Schumacher, J.C., 1999, Petrology of sapphirine-bearing and associated granulites from central Sri Lanka: Journal of Petrology, v. 40, no. 8, p. 1211–1239.

Lal, R.K., Ackermand, D., Raith, M., Raase, P., and Seifert, F., 1984, Sapphirine-bearing assemblages from Kiranur, southern India; a study of chemographic relationships in the Na_2O-FeO-MgO-Al_2O_3-SiO_2-H_2O system: Neues Jahrbuch für Mineralogie, Abhandlungen, v. 150, no. 2, p. 121–152.

Lowell, J., 1994a, A metamorphic and deformational history of the Spuhler Peak Formation, Tobacco Root Mountains, Montana [B.A. thesis]: Colorado Springs, Colorado College, 100 p.

Lowell, J., 1994b, Petrological and structural constraints on the history of the Spuhler Peak Formation near Noble Lake, Tobacco Root Mountains, Montana, *in* Wilson, M.A., ed., Seventh Keck research symposium in geology: San Antonio, Texas, p. 78–81.

Martin, J., 1996, Petrology of mafic and felsic gneisses of the Indian Creek metamorphic suite, Tobacco Root Mountains, southwestern Montana, *in* Mendelson, C.V., and Mankiewicz, C., eds., Ninth Keck research symposium in geology: Williamstown, Massachusetts, Williams College, p. 110–113.

Moecher, D.P., Essene, E.J., and Anovitz, L.M., 1988, Calculation and application of clinopyroxene-garnet-plagioclase-quartz geobarometers: Contributions to Mineralogy and Petrology, v. 100, no. 1, p. 92–106.

Mogk, D.W., Burger, H.R., Mueller, P.A., D'Arcy, K., Heatherington, A.L., Wooden, J.L., Abeyta, R.L., Martin, J., and Jacob, L.J., 2004, Geochemistry of quartzofeldspathic gneisses and metamorphic mafic rocks of the Indian Creek and Pony–Middle Mountain Metamorphic Suites, Tobacco

Root Mountains, Montana, *in* Brady, J.B., et al., eds., Precambrian geology of the Tobacco Root Mountains, Montana: Boulder, Colorado, Geological Society of America Special Paper 377, p. 15–46 (this volume).

Mohan, A., Prakash, D., and Motoyoshi, Y., 1996, Decompressional P-T history in sapphirine-bearing granulites from Kodaikanal, southern India: Journal of Southeast Asian Earth Sciences, v. 14, no. 3–4, p. 231–243.

Mohlman, H.K., 1996a, Evolution of Archean metamorphosed mafic dikes in the Tobacco Root Mountains, SW Montana [B.A. thesis]: Amherst, Massachusetts, Amherst College, 82 p.

Mohlman, H.K., 1996b, Tectonometamorphic evolution of metamorphosed mafic dikes in the Archean rocks of the Tobacco Root Mountains, Montana, *in* Mendelson, C.V., and Mankiewicz, C., eds., Ninth Keck research symposium in geology: Williamstown, Massachusetts, Williams College, p. 114–117.

Mohlman, H.K., and Cheney, J.T., 1996, Tectonometamorphic evolution of metamorphosed mafic dikes (MMD) in the Archean rocks of the Tobacco Root Mountains, Montana: Geological Society of America Abstracts with Programs, v. 28, no. 3, p. 83.

Monteleone, B., 1998a, A petrologic and mathematical analysis of metamorphism in the Indian Creek metamorphic suite and the Spuhler Peak metamorphic suite, Tobacco Root Mountains, southwestern Montana [B.A. thesis]: Wooster, Ohio, College of Wooster, 56 p.

Monteleone, B., 1998b, The petrology and geothermobarometry of the Indian Creek metamorphic suite and the Spuhler Peak metamorphic suite, Tobacco Root Mountains, southwestern Montana, *in* Mendelson, C.V., and Mankiewicz, C., eds., Eleventh Keck research symposium in Geology: Amherst, Massachusetts, Amherst College, p. 184–187.

Mueller, P.A., Burger, H.R., Wooden, J.L., Heatherington, A.L., Mogk, D.W., and D'Arcy, K., 2004, Age and evolution of the Precambrian crust of the Tobacco Root Mountains, Montana, *in* Brady, J.B., et al., eds., Precambrian geology of the Tobacco Root Mountains, Montana: Boulder, Colorado, Geological Society of America Special Paper 377, p. 181–202 (this volume).

Mukhopadhyay, B., and Bose, M.K., 1994, Transitional granulite-eclogite facies metamorphism of basic supracrustal rocks in a shear zone complex in the Precambrian shield of South India: Mineralogical Magazine, v. 58, no. 1(390), p. 97–118.

Ouzegane, K., and Boumaza, S., 1996, An example of ultrahigh-temperature metamorphism; orthopyroxene-sillimanite-garnet, sapphirine-quartz and spinel-quartz parageneses in Al-Mg granulites from In Hihaou: Journal of Metamorphic Geology, v. 14, no. 6, p. 693–708.

Patino Douce, A.E., Johnston, A.D., and Rice, J.M., 1993, Octahedral excess mixing properties in biotite; a working model with applications to geobarometry and geothermometry: American Mineralogist, v. 78, no. 1–2, p. 113–131.

Pattison, D.R.M., 2003, Petrogenetic significance of orthopyroxene-free garnet + clinopyroxene + plagioclase ± quartz-bearing metabasites with respect to the amphibolite and granulite facies: Journal of Metamorphic Geology, v. 21, no. 1, p. 21–34.

Perkins, D., and Chipera, S.J., 1985, Garnet-orthopyroxene-plagioclase-quartz barometry: Refinement and application to the English River subprovince and the Minnesota River Valley: Contributions to Mineralogy and Petrology, v. 89, p. 69–80.

Powell, R., 1985, Regression diagnostics and robust regression in geothermometer/geobarometer calibration; the garnet-clinopyroxene geothermometer revisited: Journal of Metamorphic Geology, v. 3, no. 3, p. 231–243.

Raith, M., Karmakar, S., and Brown, M., 1997, Ultra-high-temperature metamorphism and multistage decompressional evolution of sapphirine granulites from the Palni Hills Ranges, southern India: Journal of Metamorphic Geology, v. 15, no. 3, p. 379–399.

Reid, R.R., 1957, Bedrock geology of the north end of the Tobacco Root Mountains, Madison County, Montana: Montana Bureau of Mines and Geology Memoir 36, p. 27.

Reid, R.R., 1963, Metamorphic rocks of the northern Tobacco Root Mountains, Madison County, Montana: Geological Society of America Bulletin, v. 74, p. 293–305.

Rodriguez, M.L., 2002, Analysis of the relationship between strain and metamorphic equilibrium as preserved in Archean amphibolites from the Tobacco Root Mountains, Montana [B.A. thesis]: Amherst, Massachusetts, Amherst College, 72 p.

Root, F.K., 1965, Structure, petrology, and mineralogy of pre-Beltian metamorphic rocks of the Pony-Sappington area, Madison County, Montana [Ph.D. thesis]: Bloomington, Indiana University, 184 p.

Spear, F.S., 1993, Metamorphic phase equilibria and pressure-temperature-time paths, Mineralogical Society of America Monographs: Washington, D.C., Mineralogical Society of America, 799 p.

Spear, F.S., and Markussen, J.C., 1997, Mineral zoning, P-T-X-M phase relations, and metamorphic evolution of some Adirondack granulites, New York: Journal of Petrology, v. 38, no. 6, p. 757–783.

Spear, F.S., and Menard, T., 1989, Program GIBBS: A generalized Gibbs method algorithm: American Mineralogist, v. 74, p. 942–943.

Spear, F.S., and Parrish, R.R., 1996, Petrology and cooling rates of the Valhalla Complex, British Columbia, Canada: Journal of Petrology, v. 37, no. 4, p. 733–765.

Spear, F.S., Kohn, M.J., and Cheney, J.T., 1999, P-T paths from anatectic pelites: Contributions to Mineralogy and Petrology, v. 134, no. 1, p. 17–32.

Steffen, K.J., 1998a, Garnet-amphibolite geothermobarometry of the Archean metamorphic suites in the Tobacco Root Mountains, Montana; implications for crustal evolution of the northern Wyoming province: Geological Society of America Abstracts with Programs, v. 30, no. 6, p. 37.

Steffen, K.J., 1998b, Geothermbarometry of garnet-amphibolites of the Archean Spuhler Peak and Pony–Middle Mountain Metamorphic Suites of the Tobacco Root Mountains, southwest Montana [B.A. thesis]: Northfield, Minnesota, Carleton College, 101 p.

Steffen, K.J., 1998c, Geothermobarometry of Archean garnet-amphibolites; Pony–Middle Mountain and Spuhler Peak metamorphic suites, Tobacco Root Mountains, southwest Montana, *in* Mendelson, C.V., and Mankiewicz, C., eds., Eleventh Keck research symposium in Geology: Amherst, Massachusetts, Amherst College, p. 192–195.

Steiner, M.L., 1999, Metamorphic evolution of Indian Creek Metamorphic Suite garnet+orthopyroxene assemblages, Tobacco Root Mountains, Montana [B.A. thesis]: Amherst, Massachusetts, Amherst College, 93 p.

Tansley, W., Schafer, P.A., and Hart, L.H., 1933, A geological reconnaissance of the Tobacco Root Mountains, Madison County, Montana: Montana Bureau of Mines and Geology Memoir 9, p. 57.

Tierney, K.A., 1994a, The origin and evolution of the Spuhler Peak Formation along the western ridge of Thompson Peak, Tobacco Root Mountains, Montana [B.A. thesis]: Amherst, Massachusetts, Amherst College, 87 p.

Tierney, K.A., 1994b, The origin and evolution of the Spuhler Peak Formation along the western ridge of Thompson Peak, Tobacco Root Mountains, Montana, *in* Wilson, M.A., ed., Seventh Keck research symposium in geology: San Antonio, Texas, p. 94–97.

Tuit, C.B., 1996a, Geothermobarometry of the Indian Creek Metamorphic Suite, Tobacco Root Mountains, Montana: Geological Society of America Abstracts with Programs, v. 28, no. 7, p. 357–358.

Tuit, C.B., 1996b, Geothermobarometry of the Indian Creek metamorphic suite, Tobacco Root Mountains, Montana, *in* Mendelson, C.V., and Mankiewicz, C., eds., Ninth Keck research symposium in geology: Williamstown, Massachusetts, Williams College, p. 86–89.

Tuit, C.B., 1996c, Geothermometry of the Indian Creek Metamorphic Suite, Tobacco Root Mountains, Montana [B.S. thesis]: Beloit, Wisconsin, Beloit College, 43 p.

Van Reenen, D.D., 1986, Hydration of cordierite and hypersthene and a description of the retrograde orthoamphibole isograd in the Limpopo belt, South Africa: American Mineralogist, v. 71, p. 900–915.

Vitaliano, C.J., Burger, H.R., Cordua, W.S., Hanley, T.B., Hess, D.P., and Root, F.K., 1979, Explanatory text to accompany geologic map of southern Tobacco Root Mountains, Madison County, Montana: Geological Society of America Map and Chart Series MC31, scale 1:62,500, 1 sheet, 8 p. text.

Wegmann, K.W., 1996a, Metamorphic evolution of the Archean Pony Middle Mountain Metamorphic Suite, Tobacco Root Mountains, southwestern Montana [B.A. thesis]: Walla Walla, Washington, Whitman College, 74 p.

Wegmann, K.W., 1996b, Metamorphic evolution of the Archean Pony Middle Mountain metamorphic suite, Tobacco Root Mountains, southwestern Montana, *in* Mendelson, C.V., and Mankiewicz, C., eds., Ninth Keck research symposium in geology: Williamstown, Massachusetts, Williams College, p. 122–125.

Windley, B.F., Ackermand, D., and Herd, R.K., 1984, Sapphirine/kornerupine-bearing rocks and crustal uplift history of the Limpopo Belt, Southern Africa: Contributions to Mineralogy and Petrology, v. 86, p. 342–358.

Wolf, M.B., and Wyllie, P.J., 1995, Liquid segregation parameters from amphibolite dehydration melting experiments: Journal of Geophysical Research, B, Solid Earth and Planets, v. 100, no. 8, p. 15,611–15,621.

Manuscript Accepted by the Society September 12, 2003

Printed in the USA